RESEARCH PAPER

Overexpression of the receptor-like kinase *BIR1* gene causes *SOBIR1*- and *EDS1*-dependent cell death phenotypes in Arabidopsis

Irene Guzmán-Benito[1,2], Carmen Robinson[1,3], Isabel Punzón[1], César Llave[1,*]

1. Centro de Investigaciones Biológicas Margarita Salas. Consejo Superior de Investigaciones Científicas, Ramiro de Maeztu 9, 28040 Madrid, Spain
2. Current address. Department of Plant Molecular Biology, University of Lausanne, 1015 Lausanne, Switzerland
3. Doctorado en Biotecnología y Recursos Genéticos de Plantas y Microorganismos Asociados, Universidad Politécnica de Madrid, 28040 Madrid, Spain

*Author for correspondence: cesarllave@cib.csic.es (C.L.)

ABSTRACT: 196
WORD COUNT: 6,894

Number of figures: 8
Number of figures in color: 8

Supporting information:
Number of Supporting figures: 8
Number of Supporting tables: 8

ORCIDS

Irene Guzmán-Benito	0000-0002-9912-8164
Carmen Robinson	0000-0002-7146-0253
César Llave	0000-0003-3844-4582

Abstract

The receptor-like kinase *BAK1-INTERACTING RECEPTOR-LIKE KINASE 1* (*BIR1*) functions as a negative regulator of multiple resistance signaling pathways in *Arabidopsis thaliana*. Previous studies showed that loss of *BIR1* function leads to extensive cell death and activation of constitutive immune responses. Here, we use a dexamethasone (DEX)-inducible expression system to investigate the impact of *BIR1* overexpression on plant growth and development and immune regulation. We show that, in the absence of microbes or microbe-derived elicitors/effectors, plants that overexpress *BIR1* displayed cell death phenotypes that concur with the transcriptomic up-regulation of multiple immune pathways involved in pathogen perception and defense signal transduction. *BIR1* overexpression has similar loss-of-function effects to *BIR1* depletion in knockout plants, which suggests that proper *BIR1* homeostasis requires a tight regulation of *BIR1* expression within a functional threshold. We show that *ENHANCED DISEASE SUSCEPTIBILITY 1* (*EDS1*) and *SUPPRESSOR OF BIR1-1* (*SOBIR1*) are required for the effector-triggered immunity (ETI)-type cell death phenotypes associated with overexpression of *BIR1*. Our data is then consistent with the current hypothesis by which loss of *BIR1* regulation and/or integrity is sensed by one or several guarding resistance (NLR) proteins to initiate a cell death response, in which SOBIR1 cooperates with EDS1 to transduce signals downstream of R proteins.

Running head

Effects of *BIR1* overexpression on plant immunity and development

Key words

Arabidopsis, BAK1-INTERACTING RECEPTOR-LIKE KINASE 1 (BIR1), cell death, ENHANCED DISEASE SUSCEPTIBILITY 1 (EDS1), immune regulation, effector-triggered immunity, pattern-triggered immunity, SUPPRESSOR OF BIR1 (SOBIR1)

Summary Statement

Regulation of the receptor-like kinase *BIR1* has a strong impact on plant growth and development and immune homeostasis in Arabidopsis. *BIR1* overexpression causes cell death-

60 and senescence-like phenotypes that require *EDS1* and *SOBIR1* signaling pathways, and that
61 resemble to those observed by *BIR1* depletion.

62 # 1 INTRODUCTION

63 Plants use immunity to defend themselves against invaders such as bacteria, fungi, oomycetes,
64 and viruses (Korner *et al.*, 2013; Nishad *et al.*, 2020). Pattern-triggered immunity (PTI) uses
65 multiple cell-surface pattern recognition receptors (PRR) to recognize
66 pathogen/microbe/damage-associated molecular patterns (PAMP/MAMP/DAMP). Effector-
67 triggered immunity (ETI) involves intracellular receptors that sense pathogen-effector proteins
68 or effector-induced manipulations of host proteins (Zhou & Zhang, 2020; Yu *et al.*, 2021).
69 PRRs are single-transmembrane receptor-like kinases (RLK) or receptor-like proteins (RLP).
70 PRRs form active receptor complexes in a ligand-dependent manner with members of the
71 somatic embryogenesis co-receptor kinases (SERKs), including BRASSINOSTEROID
72 INSENSITIVE1-ASSOCIATED RECEPTOR KINASE 1 (BAK1/SERK3) (Boutrot & Zipfel,
73 2017; Hohmann *et al.*, 2017; Smakowska-Luzan *et al.*, 2018). BAK1 functions as a positive
74 regulator of PTI (Wu *et al.*, 2020), and has a dual role as positive and negative regulator of cell
75 death during ETI (Belkhadir *et al.*, 2012; Dominguez-Ferreras *et al.*, 2015). RLP-type PRRs
76 lack kinase activity and constitutively associate in a ligand-independent manner with the
77 leucine-rich repeat (LRR)-RLK SUPPRESSOR OF BIR1-1 (SOBIR1) (Gust *et al.*, 2017). Once
78 the microbe is sensed, PRR complexes activate receptor-like cytoplasmic kinases (RLCKs) that
79 initiate downstream signaling cascades (Liang & Zhou, 2018; Rao *et al.*, 2018). Among them,
80 BOTRYTIS INDUCED KINASE1 (BIK1) functions as a positive regulator of immunity when
81 triggered by LRR-RLKs or as a negative regulator when triggered by LRR-RLPs (Bi *et al.*,
82 2018; Wan *et al.*, 2019).

83 ETI relies on nucleotide-binding domain LRR intracellular immune receptors (NLRs) encoded
84 by polymorphic disease resistance genes. NLRs comprise either proteins with an N-terminal
85 domain similar to the TOLL/INTERLEUKIN RECEPTOR 1 (TIR1) (TIR-NB-LRR, TNL),
86 proteins with a coiled-coil (CC) domain at the N terminus (CC-NB-LRR, CNL) or proteins with
87 a RESISTANCE TO POWDERY MILDEW 8-LIKE DOMAIN (RPW8)-type domain (RNLs)
88 (van Wersch *et al.*, 2020; Wang & Chai, 2020). NLRs function as "sensors" that recognize
89 effectors, or as "helpers" that mediate signaling downstream of sensor NLRs (Jubic *et al.*,
90 2019). Recent studies demonstrated that PTI and ETI work together to mutually potentiate the
91 immune response (Yuan *et al.*, 2021b; Yuan *et al.*, 2023). NLR-mediated signaling is dependent
92 on multiple PTI-associated components such as BAK1, SOBIR1, or BIK1 in a PTI-independent
93 manner, while TNL-coding genes that are up-regulated during early PTI boost immune
94 responses (Ngou *et al.*, 2021; Tian *et al.*, 2021; Yuan *et al.*, 2021a). ENHANCED DISEASE

95 SUSCEPTIBILITY (EDS1) and PHYTOALEXIN DEFICIENT 4 (PAD4), which are essential
96 in TNL-mediated immunity, also play a key role in PTI signaling in response to different
97 microbial elicitors (Pruitt *et al.*, 2021b; Tian *et al.*, 2021). Furthermore, PTI and ETI outputs
98 usually converge, albeit with different amplitude and duration (Yuan *et al.*, 2021b). Early
99 immune responses include apoplastic reactive oxygen species (ROS) burst, cytosolic calcium
100 (Ca^{+2}) influx and activation of Ca^{+2}-dependent protein kinases (CPK), and activation of
101 mitogen-activated protein kinases (MAPK). This response is followed by the transcriptional
102 activation of defense processes that include accumulation of defense phytohormones, regulation
103 of cell wall and secretome composition alteration (Li *et al.*, 2020).

104 Plants deploy a variety of mechanisms to avoid the detrimental effects of hyperactivated
105 defenses (Couto & Zipfel, 2016; Withers & Dong, 2017; Mithoe & Menke, 2018). Among
106 them, BAK1-INTERACTING RECEPTOR-LIKE KINASE (BIR) proteins play a key role in
107 defense attenuation. The current model postulates that, in the absence of microbes, BIR proteins
108 constitutively associate with BAK1, maintaining the PRRs in a resting state. During ligand
109 perception, BAK1 dissociates from BIR and becomes accessible to complex with PRR
110 receptors (Gao *et al.*, 2009; Halter *et al.*, 2014; Imkampe *et al.*, 2017). The Arabidopsis genome
111 contains four *BIR* homologs. *BIR1* negatively regulates cell death signaling pathways that
112 depend on BAK1, SOBIR1, EDS1 and PAD4, and that likely involve components of the TNL-
113 mediated ETI response (Gao *et al.*, 2009; Schulze *et al.*, 2022). Arabidopsis *BIR2* and *BIR3*
114 have critical roles in repressing PRR-mediated PTI responses (Halter *et al.*, 2014; Imkampe *et*
115 *al.*, 2017). Furthermore, the TNL protein CSA1 interacts physically with BIR3 and senses
116 perturbances in the BIR3/BAK1 complex to induce cell death (Schulze *et al.*, 2022). *BIR4* has
117 so far not been characterized.

118 *BIR1* expression is transcriptionally activated by multiple microbial and viral pathogens in a
119 salicylic acid (SA)-dependent manner (Guzman-Benito *et al.*, 2019). Under normal conditions,
120 the *BIR1* gene undergoes transcriptional negative regulation by RNA-directed DNA
121 methylation whereas a potent site-directed post-transcriptional silencing dynamically reinforces
122 the action of the epigenetic regulation when *BIR1* is transcriptionally activated (Guzman-Benito
123 *et al.*, 2019). RNA silencing is thus a critical mechanism for the maintenance of *BIR1*
124 homeostasis. Indeed, we previously showed that overexpression of either a human influenza
125 hemagglutinin (HA)- or a mCherry-tagged version of *BIR1* using a *Tobacco rattle virus* (TRV)-
126 based expression system or a transgenic dexamethasone (DEX)-inducible system, respectively,
127 produced a range of senescence and cell death phenotypes in Arabidopsis (Guzman-Benito *et*

128 *al.*, 2019). Whereas the autoimmune response in *bir1-1* knockout mutants has been extensively
129 characterized (Gao *et al.*, 2009; Liu *et al.*, 2016), little is known about the molecular basis of
130 the phenotypes associated to an excess of *BIR1*. In this work, we use a previously characterized
131 DEX-inducible system in Arabidopsis to investigate the immune components and pathways
132 responsible for the phenotypes associated with *BIR1* gene overexpression in the absence of
133 microbes or microbe-derived elicitors/effectors. We found that senescence and cell death-like
134 phenotypes in *BIR1* overexpressing lines coincide with an inadequate overexpression of genes
135 encoding immune receptors and co-receptors involved in the perception and downstream
136 signaling of ligands and effectors, which resemble those observed in *BIR1* knockout plants. We
137 evaluated the effects of the genetic depletion of several master regulators of the immune
138 response and found that the cell death phenotypes associated with *BIR1* overexpression require
139 the TNL-associated EDS1 and/or the RLP-co-receptor SOBIR1, but the underlying mechanism
140 is unknown.

141

142 # 2 METHODS

143 ## 2.1 Plant material and growth condition

144 *Arabidopsis thaliana* plants were grown in controlled environmental chambers under long-day
145 conditions (16h day/8h night) at 22°C. Arabidopsis lines used in this study were derived from
146 the Columbia-0 (Col-0) ecotype. Seeds were surface-sterilized and sown on plates containing
147 ½ Murashige and Skoog (MS) medium supplemented with MES (0,5g/L), 1% sucrose and 0,9%
148 Plant agar (Duchefa Biochemie). Seedlings were transferred to soil 7 to 10 days after
149 germination.

150 Mutants for *bir1-1* and *sobir1-12* were donated by Yuelin Zhang (University of British
151 Columbia, Canada). The *eds1-2*, *pad4-1* and *eds5-3* alleles were supplied by Jane E. Parker
152 (Max Planck Institute for Plant Breeding Research, Germany). Mutant *bak1-5* was donated by
153 Birgit Kemmerling (Center of Plant Molecular Biology, University of Tübingen, Germany).
154 The *sid2-2* mutant was a gift from Francisco Tenllado (Centro de Investigaciones Biológicas
155 Margarita Salas, CSIC, Spain). All Arabidopsis plants used in this study were in the Col-0
156 background.

157 Arabidopsis transgenic plants expressing a BIR1-mCherry fusion under a dexamethasone
158 (DEX)-inducible gene expression system (BIR1 L6 and BIR1 L9) were previously described
159 (Guzman-Benito *et al.*, 2019). The same DEX-inducible expression system containing a

160 mCherry-tagged *BIR1* gene was transformed into Arabidopsis mutant backgrounds according
161 to standard floral dipping (Clough & Bent, 1998). Independent homozygous lines were selected
162 in T3 and used for subsequent experiments. Morphological phenotypes after DEX treatments
163 were investigated in at least two independent transgenic lines of each genotype.

164

165 ## 2.2 RNA and Protein analyses

166 Total RNA was extracted using TRIzol reagent (Invitrogen) and treated with DNase I
167 (Invitrogen) following manufacturer's instructions to eliminate genomic DNA traces. One-step
168 quantitative RT-PCR (RT-qPCR) was carried out using Brilliant III Ultra-Fast SYBR Green
169 QRT-PCR Master Mix (Agilent Technologies) in a Rotor-Gene 6000/Rotor-Gene Q real-time
170 PCR machine (Corbett/Qiagen) (Fernandez-Calvino *et al.*, 2016). Relative gene expression was
171 determined using the Delta-delta cycle threshold method and Rotor-Gene 6000 Series Software
172 (Corbett). Transcript levels of the target genes were normalized to the transcript levels of the
173 housekeeping gene *CBP20* (*At5g44200*) as a reference gene. Gene-specific primers are given
174 in Table S1.

175 For protein analyses, leaf tissue samples were ground in liquid nitrogen and homogenized in
176 extraction buffer (65 mM Tris-HCl, pH 8; 3% sodium dodecyl sulfate [SDS]; 1% ß-
177 mercaptoethanol; 10% glycerol). Samples were diluted in Laemmli buffer, incubated for 5 min
178 at 95°C, and loaded onto 10% SDS-PAGE protein gels. After electrophoresis, proteins were
179 blotted onto an ECL nitrocellulose membrane (Amersham-Pharmacia), and detected using
180 commercial horseradish peroxide (HRP)-conjugated secondary antibodies and a
181 chemiluminescent substrate (LiteAblot Plus).

182

183 ## 2.3 Library preparation for transcriptome sequencing and bioinformatic analyses

184 Total RNA was extracted from each sample using the RNeasy plant mini kit (Qiagen) followed
185 by DNase treatment according to manufacturer's instructions. Each sample consisted of RNA
186 pooled from six individual plants. The RNA purity and RNA concentration were checked using
187 a Nanodrop spectrophotometer (ThermoFisher Scientific), while the RNA integrity was
188 measured using the Agilent Bioanalyzer 2100 system (Agilent Technologies). Sequencing
189 libraries were generated at NOVOGENE (HK) COMPANY LIMITED (Wan Chai, Hong
190 Kong) (www.novogene.com) using NEBNext® UltraTM RNA Library Prep Kit for Illumina®

191 (New England Biolabs) following manufacturer's recommendations and index codes were
192 added to attribute sequences to each sample. First-strand cDNA from mRNA was synthesized
193 using random hexamer primer and M-MuLV Reverse Transcriptase (RNase H-). Second-strand
194 cDNA synthesis was subsequently performed using DNA Polymerase I and RNase H.
195 NEBNext Adaptors with hairpin loop structure were ligated. In order to select cDNA fragments
196 of preferentially 150~200 bp in length, the library fragments were purified with the AMPure
197 XP system (Beckman Coulter). PCR was done with Phusion High-Fidelity DNA polymerase,
198 Universal PCR primers and Index (X) Primer. PCR products were purified with the AMPure
199 XP system and library quality was assessed on the Agilent Bioanalyzer 2100 system. Clustering
200 of the index-coded samples was performed on a cBot Cluster Generation System using the
201 TruSeq PE Cluster Kit v3-cBot-HS (Illumina) according to the manufacturer's
202 recommendations. Finally, paired-end reads were generated via an Illumina PE150 Hiseq
203 platform at NOVOGENE (HK) COMPANY LIMITED.

204 Clean reads were obtained by removing adaptor tags and reads containing poly-N and low-
205 quality reads from raw data. Paired-end clean reads were mapped to the Arabidopsis TAIR v10
206 reference genome using HISAT2 software. To quantify the gene expression levels, HTSeq
207 v0.6.1 was used to calculate the number of mapped reads of each gene and then normalize the
208 results to the expected number of Fragments Per Kilobase of transcript sequence per Millions
209 of base-pairs sequenced (FPKM). Differential expression analysis between groups (three
210 biological replicates per condition) was performed using DESeq2 R package (1.18.0). The
211 resulting *p-value*s were adjusted using the Benjamini and Hochberg's approach for controlling
212 the False Discovery Rate (FDR). Genes with an adjusted *p-value* ≤0.05 found by DESeq2 were
213 deemed as differentially expressed (DEG). Functional classification of DEGs including Gene
214 Ontology (GO) and KEGG was performed. GO enrichment analysis of DEGs was implemented
215 by tGOseq R package, in which gene length bias was corrected. KOBAS software was used to
216 test the statistical enrichment of DEGs in the KEGG database GO terms and KEGG pathways
217 with corrected *p-value* ≤0.05 were considered significantly enriched by DEGs. The raw data
218 was deposited in the Gene Expression Omnibus under accession number GSE234036.

219

220 2.4 Dexamethasone (DEX) treatments and sampling procedure.

221 DEX (Sigma) was dissolved in 100% ethanol to make a 30 mM DEX stock solution which was
222 stored at –20°C in a light-tight vial. Arabidopsis plants were grown for three to four weeks in

223 soil and sprayed at 24 h intervals with DEX at 30 µM as indicated (McNellis *et al.*, 1998). At
224 this concentration, plants display optimal induction of the transgene (Guzman-Benito *et al.*,
225 2019). Samples for gene expression assays were collected at the outset of symptoms
226 appearance, which normally corresponded to approximately 12 days of DEX treatments. This
227 time however could differ between genotypes and treatments and consequently plants of each
228 genotype may exhibit different ages and developmental stages when harvested compared to
229 each other genotypes. As a result, quantitative comparisons and inferences on gene expression
230 levels between genotypes should be made with caution in this study.

231

232 # 3 RESULTS

233 ## 3.1 *BIR1* overexpression causes transcriptome reprogramming in Arabidopsis

234 We conducted a transcriptomic analysis of Arabidopsis BIR1 L9 plants, which express a DEX-
235 inducible *BIR1-mCherry* transgene (hereafter *BIR1*) (Guzman-Benito *et al.*, 2019), to
236 understand the downstream biological processes and pathways associated with *BIR1*
237 overexpression. This system proves to be a valuable tool for studying *BIR1* effects in the
238 absence of pathogen elicitors or effectors. After DEX treatment, BIR1 L9 plants start showing
239 morphological and growth defects from approximately day 12 onward, including severe
240 stunting, leaf deformation, premature senescence (yellowing), and cell death (Figure 1a)
241 (Guzman-Benito *et al.*, 2019). At this time, we detected roughly two orders of magnitude more
242 mCherry-tagged BIR1 protein than after four days of DEX treatment, indicating that BIR1
243 protein accumulates gradually overtime in DEX-treated BIR1 L9 plants (Figure 1a). These
244 phenotypes were identical to those observed when a BIR1-HA-coding construct was
245 systemically overexpressed in Arabidopsis plants using a TRV-based expression system
246 (Figure 1a) (Guzman-Benito *et al.*, 2019). Hence, we can confidently attribute the observed cell
247 death phenotypes to overexpression of *BIR1* and not to DEX side-effects or protein tagging.
248 Under our experimental conditions, and consistent with previous studies, DEX caused a
249 moderate growth retardation in WT plants when applications began at an early growth stage
250 (Boyes stage 1.5), whereas DEX caused no growth defects when applied at later stages of plant
251 development (Boyes stage 1.7) (Figure 1a, S1a) (Boyes *et al.*, 2001; Ouwerkerk *et al.*, 2001).
252 In no case, WT plants exhibited cell death or morphological phenotypes upon DEX treatment
253 (Figure 1a, S1a).

254 For RNA-seq, three-week-old plants were sprayed with DEX for 12 days whereas control plants
255 were mock-treated with H_2O. Three biological replicates were used as representative samples
256 of each condition tested in this study: DEX-treated WT (DeWT_), mock-treated WT (MoWT_),
257 DEX-treated BIR1 L9 (DeL9_) and mock-treated BIR1 L9 (MoL9_) plants as indicated (Table
258 S2). To avoid extensive damage on the plant transcriptome, RNA seq samples were collected
259 before the onset of cell death symptoms. Our data indicate that *BIR1* overexpression triggered
260 a massive transcriptional reprogramming in Arabidopsis (Figure 1b) (Table S2)**.** Differentially
261 expressed genes (DEG) from different comparisons are presented in Table S3. DEGs using
262 different statistical thresholds are shown in Figure S2a,b and Table S4.

263 Principal component analysis (PCA) was used to sort RNA-seq-based transcriptomic data
264 according to gene expression levels. PC1 clearly separated the DEX-treated BIR1 L9 samples
265 (DeL9_12) from the other conditions in the PCA score plot after 12 days of treatment, indicating
266 that the *BIR1* expression level was the main source of variance (28.37%) (Figure 1c). WT
267 samples, irrespective of DEX treatment, and mock-treated BIR1 L9 samples clustered in their
268 proximity, reflecting similar gene expression profiles (Figure 1c). This result also suggested
269 that DEX alone was not a major contributor of the transcriptomic changes observed in DEX-
270 treated BIR1 L9 samples. PC2 highlights a shift in gene expression between samples due to age
271 or developmental stage (16.83%) (Figure 1c). Samples of both genotypes collected after 4 days
272 of DEX treatments were located close each other in the score plot, suggesting that, under this
273 induction conditions, *BIR1* has a minimal impact on gene expression. Intriguingly, the
274 DeL9_12b sample was located far from the other DeL9_12 samples in the PCA plot, and near
275 the samples within the DeWT_12, MoWT_12 or MoL9_12 groups (Figure 1c). The levels of
276 *BIR1* induction in the replicate DeL9_12b was substantially lower than in the other two
277 replicates within the DeL9_12 group (Figure 1d). This observation implies that a lower
278 overexpression of *BIR1* in the DeL9_12b sample has much less impact on the plant
279 transcriptome than a higher overexpression as shown for the other two DeL9_12 replicates.

280 Gene ontology (GO) analysis showed that genes encoding proteins with oxidoreductase
281 activity, transmembrane transport and other metabolic processes or genes related to lipid or
282 carbohydrate metabolism were particularly overrepresented in our whole set of DEGs,
283 including WT and BIR1 L9 plants **(**Figure 1e, S2c**)** (Table S5). These alterations on the plant
284 transcriptome were presumably DEX-dependent. In contrast, DEGs with kinase activity were
285 only enriched in *BIR1* overexpressing plants, relative to mock-treated BIR1 L9 plants **(**Figure
286 1e and S2c**)** or DEX-treated WT plants (Figure S1c). The Kyoto Encyclopedia of Genes and

287 Genomes (KEGG) pathway analysis showed the enrichment of genes related to several
288 metabolic processes and genes involved in the biosynthesis of secondary metabolites that were
289 specifically activated after DEX-treatments (Figure S3) (Table S6). Conversely, DEGs
290 involved in plant hormone signal transduction were significantly enriched only in DEX-treated
291 BIR1 L9, but not in mock-treated BIR1 L9 plants or DEX-treated WT plants.

292

293 3.2 *BIR1* overexpression triggers the expression of immunity-related genes

294 RNA-Seq results were further validated in mock- and DEX-treated BIR1 L9 plants after 12
295 days of treatment using RT-qPCR. We found that expression of DEGs *BIR1*, *PR1*,
296 *RESPIRATORY BURST OXIDASE HOMOLOG PROTEIN D* (*RBOHD*), *FRK1* and
297 *CYTOCHROME P450 MONOOXYGENASE 79B2* (*CYP79B2*) were all up-regulated in
298 Arabidopsis plants overexpressing *BIR1* compared to mock-treated controls. This finding is
299 consistent with their RNA-Seq-based profiles and confirms reproducibility in their expression
300 patterns (Figure 2a).

301 A detailed inspection of the RNA-Seq data revealed that multiple genes involved in the
302 perception of pathogens and the activation of defense pathways were misregulated when *BIR1*
303 was overexpressed, but not in DEX-treated WT plants or mock-treated BIR1 L9 transgenic
304 plants [$|\log_2$ (Fold-Change)$| \geq 1$ and adjusted *p*-value ≤ 0.01] (Table S4). Two-tailed Fisher's
305 exact tests revealed that genes encoding LRR-type RLKs in the Arabidopsis genome were
306 significantly enriched (Table S8). Particularly**,** genes encoding cysteine-rich RLKs (CRK),
307 which likely are important in the perception of apoplastic ROS and in the activation of PTI and
308 cell death, were overrepresented in the pool of DEGs (Figure 2b) (Table S7) (Chen, 2001; Yeh
309 *et al.*, 2015; Quezada *et al.*, 2019; Castro *et al.*, 2021). Interestingly, inspection of transcript
310 abundance in single replicates indicated that the differential expression of CRK-coding genes
311 was closely related to *BIR1* levels (Figure 2c). We also detected a high percentage of PRRs of
312 the RLP class, not expected by chance, in the list of DEGs, being their relative transcript
313 abundance consistent with *BIR1* expression levels (Figure 3a,b) (Table S7) (Wang *et al.*, 2008;
314 Lv *et al.*, 2016). RLPs have been observed to be predominantly expressed in plants undergoing
315 leaf senescence, supporting the idea that *BIR1* overexpression accelerates a senescence program
316 (Wang *et al.*, 2008). In Arabidopsis, *RLP23*, *RLP30*, and *RLP42* genes mediate SOBIR1-
317 dependent immune activation, but the role of other RLPs in the perception of pathogen and
318 defense is unknown (Wang *et al.*, 2008; Zhang *et al.*, 2013; Albert *et al.*, 2019) (Table S7).

319 Conversely, PRRs of the RLK class known for eliciting immune responses were not collectively
320 and significantly up-regulated in *BIR1* overexpressing plants (Figure S4a). For instance, the
321 leucine-rich repeat RLK *ELONGATION FACTOR-TU RECEPTOR* (*EFR*) was up-regulated,
322 whereas *FLAGELLING SENSING 2* (*FLS2*) or *PEP1 RECEPTOR 1* (*PEPR1*) and *PEPR2*,
323 which sense danger-associated AtPeps (Krol *et al.*, 2010), or *MDIS1-INTERACTING*
324 *RECEPTOR LIKE KINASE 2* (*MIK2*), which recognizes conserved signature from
325 phytocytokines and microbes (Hou *et al.*, 2021), showed no responsiveness to *BIR1*
326 overexpression. Among the lysin motif (LysM) RLK family (LYK), *LYK5* (Wan *et al.*, 2012;
327 Cao *et al.*, 2014), or *LYSM DOMAIN GPI-ANCHORED PROTEIN 1* (*LYM1*), which perceives
328 peptidoglycans from the bacterial cell wall (Willmann *et al.*, 2011), were up-regulated in DEX-
329 treated BIR1 L9 plants. In contrast, *LYK4* or *LYM2* displayed no responsiveness (Faulkner *et*
330 *al.*, 2013). The expression of the genes encoding lectin RLKs *LIPOOLIGOSACCHARIDE-*
331 *SPECIFIC REDUCED ELICITATION* (*LORE*) (Luo *et al.*, 2020) and *RESISTANT TO DFPM*
332 *INHIBITION OF ABA SIGNALING 2* (*RDA2*) (Kato *et al.*, 2022) was not affected by *BIR1*
333 overexpression. Finally, we observed up-regulation of genes encoding the cell wall-associated
334 kinases (WAK), *WAK1* and *WAK2*, which contain several extracytoplasmic epidermal growth
335 factor (EGF) and recognize oligogalacturonides (He *et al.*, 1996; Brutus *et al.*, 2010).

336 In addition, *BIR1* overexpression boosted the transcription of many other genes involved in PTI
337 and ETI signaling in a dose-dependent manner too (Figure 4a). This includes the RLK co-
338 receptors *BAK1*, *SOBIR1* or *CERK1*, and RLCKs such as *BIK1* and several *AvrPphB*
339 *SUSCEPTIBLE1(PBS1)-LIKE* (*PBL*) kinases (*PBL4*, *PBL12*, *PBL20*) (Liang & Zhou, 2018;
340 Rao *et al.*, 2018) (Table S7). Active BIK1 positively regulates the Ca^{2+} influx from the apoplast
341 to the cytosol, which switches on the kinase activity of CPKs (Li *et al.*, 2014; Yip Delormel &
342 Boudsocq, 2019). Collectively, CPKs were not differentially regulated, but many genes
343 encoding individual CPKs were regarded as DEGs in plants overexpressing *BIR1* (Table S3).
344 For instance, the expression of *CPK4-6* and *CPK11* genes, which are key players in
345 transcriptional reprogramming upon elicitor perception, was enhanced only in DEX-treated
346 BIR1 L9 plants (Figure S5) (Boudsocq *et al.*, 2010). Upon ligand perception, BIK1 dissociates
347 from activated receptor complexes and phosphorylates the plasma membrane NADPH oxidase
348 RBOHD to generate extracellular ROS (Kadota *et al.*, 2014; Li *et al.*, 2014). *RBOHD* was
349 induced in DEX-treated BIR1 L9 plants, but not in their corresponding controls (Figure 4a).
350 Genes encoding lipase-like proteins *EDS1*, *PAD4*, *SENESCENCE ASSOCIATED-GENE 101*
351 (*SAG101*) and *ACTIVATED DISEASE RESISTANCE 1* (*ADR1*), which are required for TNL-

352 receptor function during ETI, were also up-regulated (Figure 4a) (Table S3) (Zhou & Zhang,
353 2020; Ngou *et al.*, 2021; Pruitt *et al.*, 2021b; Sun *et al.*, 2021; Tian *et al.*, 2021). Interestingly,
354 a large number of DEGs in our assay were annotated as resistance protein-coding genes, of
355 which the TNL class was particularly enriched in *BIR1* overexpressing plants (Swiderski *et al.*,
356 2009) (Table S7). Conversely, neither *NON-RACE SPECIFIC DISEASE RESISTANCE 1*
357 (*NDR1*) nor genes encoding CNL intracellular receptors, which require *NDR1*, were
358 differentially expressed in response to *BIR1* overexpression (Figure 4a) (Table S3). *EDS5,* an
359 important regulator of SA biosynthesis in Arabidopsis (Nawrath *et al.*, 2002), was up-regulated
360 in DEX-treated BIR1 L9 samples.

361 Interestingly, *BIR1* overexpression led to up-regulation of the *BIR2* gene, whereas *BIR3* and its
362 partner *CONSTITUTIVE SHADE AVOIDANCE 1* (*CSA1*) genes were unaffected (Figure 4a)
363 (Schulze *et al.*, 2022). Finally, transcripts of plant heterotrimeric G proteins *ARABIDOPSIS G*
364 *PROTEIN α-SUBUNIT1* (*GPA1*), *ARABIDOPSIS G PROTEIN β-SUBUNIT 1* (*AGB1*),
365 *ARABIDOPSIS G PROTEIN γ-SUBUNIT 2* (*AGG2*), and *EXTRA-LARGE G PROTEIN 1* and *2*
366 (*XLG1/2*) were more abundant in plants overexpressing *BIR1* relative to controls after 12 days
367 of DEX treatment (Figure S6). Proteins encoded by these genes positively regulate stomatal
368 defense and PTI signaling, ROS production and BIK1 stability allowing optimal immune
369 activation (Liang *et al.*, 2016; Zhong *et al.*, 2019). Differential expression of immune-related
370 genes occurred in *BIR1* overexpressing plants but not in DEX-treated WT plants, which discard
371 a potential masking effect of DEX on defense gene expression. Consistent with transcript levels,
372 SOBIR1, PAD4-dependent PR1 and EDS1 proteins were strongly up-regulated by *BIR1*
373 overexpression in DEX-treated BIR1 L9 plants, compared to the non-treated controls (Figure
374 S4b).

375 In conclusion, in the absence of microbes or microbe-derived elicitors/effectors, *BIR1*
376 overexpression drastically interferes with the immune homeostasis, causing an inadequate
377 overexpression of genes encoding immune receptors, particularly RLP and TNL receptors, and
378 co-receptors involved in the perception and downstream signaling of ligands and effectors. We
379 propose that the cell death-like phenotypes caused by *BIR1* overexpression, which are
380 reminiscent of those observed when *BIR1* function is lost, are due to an intrinsic deregulation
381 of multiple defense and resistance pathways.

382

383 ## 3.3 Genetic disruption of *SOBIR1*, but not *BAK1*, partially rescues *BIR1*
384 overexpression phenotypes

385 To understand the genetic basis of the phenotypes associated to *BIR1* overexpression, in the
386 following sections, we examined if mutations in key components of PTI and ETI signaling
387 alleviate the cell death-type morphologies and up-regulation of immune genes (Rodriguez *et*
388 *al.*, 2016; Freh *et al.*, 2022). The DEX-inducible BIR1-mCherry-coding cassette was
389 transformed into the different mutant backgrounds tested in this study. To overcome potential
390 insertion position effects, two independent BIR1-mCherry transgenic lines of each mutant
391 genotype were monitored. Phenotypes resulting from *BIR1* overexpression described in this
392 work were consistently reproduced for each mutant in both independent transgenic lines and
393 between experiments (Figure S7a,b). None of the morphological and growth defects observed
394 in transgenic BIR1 L9 overexpressing *BIR1* occurred in the mutant controls (without the
395 inducible BIR1-mCherry construct) or in a transgenic line with a mCherry-coding transgene
396 after DEX treatments (Figure S8). These controls further discard that the observed phenotypes
397 were caused by DEX treatments and/or mCherry overexpression (Figure S8).
398 *SOBIR1* and *BAK1* are necessary for activating cell death and constitutive defense responses in
399 the *bir1-1* mutant (Gao *et al.*, 2009; Liu *et al.*, 2016). To test if they were also required for the
400 *BIR1* phenotypes, we transformed the DEX-inducible BIR1-mCherry cassette into the *sobir1-*
401 *12* and *bak1-5* mutants (Gao *et al.*, 2009; Schwessinger *et al.*, 2011). Plants were sprayed with
402 DEX to trigger *BIR1* overexpression, or H_2O as control. Western blot analysis showed that
403 *sobir1-12* BIR1 and *bak1-5* BIR1 mutants accumulated as much BIR1-mCherry protein as
404 BIR1 L9 plants after 7 days of DEX treatments, indicating similar expression of the *BIR1*
405 transgene (Figure 5a). Consistent with previous results, BIR1 L9 plants, used as reference set
406 throughout the experiment, displayed severe stunting, accelerated senescence (yellowing) and
407 cell death, and accumulated abnormally high levels of *BIR1* transcripts after 12 days of DEX
408 treatment (Figure 5a,c). Localized cell death in the *BIR1* overexpressing inducible system was
409 previously shown using trypan blue staining (Guzman-Benito *et al.*, 2019). When *BIR1* was
410 overexpressed in the *sobir1-12* mutant, we observed milder phenotypes than those in BIR1 L9
411 plants, indicating that the *sobir1-12* mutation partially suppresses the morphological defects
412 associated to *BIR1* overexpression (Figure 5b**,** S7a,b). *BIR1* transcripts levels in these same
413 *sobir1-12* BIR1 plants remained strongly elevated (Figure 5c, S7c). The increased accumulation
414 of transcripts of the PTI-markers *RBOHD*, *FRK1* and *WRKY DNA-BINDING PROTEIN 29*
415 (*WRKY29*) observed upon *BIR1* overexpression was also drastically reduced in DEX-treated

416 *sobir1-12* BIR1 plants (Figure 5d). These findings indicate that *BIR1* overexpression activates
417 immune signaling pathways that require *SOBIR1*. *bak1*-5 BIR1 transgenic plants showed strong
418 morphological phenotypes and severe yellowing after 12 days of DEX application (Figure 5b,
419 S7a,b). In the set of i*bak1*-5 BIR1 plants shown in Figure 5b, *BIR1* transcript levels were only
420 moderate (Figure 5c), but remained as high as in BIR1 L9 plants in other experimental
421 repetitions (Figure S7c). *RBOHD*, *FRK1* and *WRKY* genes remained transcriptionally up-
422 regulated in DEX-treated *bak1-5* BIR1 plants although at varying degrees (Figure 5e).
423 Collectively, these data indicate that the morphological phenotypes and, perhaps, PTI gene
424 activation, observed when *BIR1* is overexpressed are genetically unrelated to *BAK1*.

425

426 3.4 Genetic disruption of *EDS1*, but not *PAD4*, partially rescues *BIR1* 427 overexpression phenotypes

428 A previous report showed that stunting, activation of cell death and defense responses in the
429 *bir1-1* mutant are partially dependent on *EDS1* and *PAD4* (Gao *et al.*, 2009). The EDS1-PAD4
430 node mediates both PTI and ETI through PRR signaling and TNL activation (Pruitt *et al.*,
431 2021a). To test if *BIR1* overexpression phenotypes were dependent on *EDS1* or *PAD4*, the
432 DEX-inducible BIR1-mCherry system was used to generate homozygous transgenic lines from
433 *eds1-2* and *pad4-1* mutants (Parker *et al.*, 1996; Zhou *et al.*, 1998). The resulting *eds1-2* BIR1
434 and *pad4-1* BIR1 plants produced comparable amounts of BIR1-mCherry protein to the BIR1
435 L9 control after 7 days of DEX applications (Figure 6a). After 12 days of DEX treatment, the
436 *eds1-2* BIR1 plants displayed mostly WT-like appearance and, occasionally, localized
437 yellowing after DEX, indicating that *eds1-2* can partially rescue the *BIR1* overexpression
438 morphologies (Figure 6b, S7a**)**. RT-qPCR analysis showed elevated levels of *BIR1* transcripts
439 in these DEX-treated *eds1-2* BIR1 plants (Figure 6c). Since TNL-coding transcripts were
440 abundant in *BIR1* overexpressing plants, we speculated that *EDS1*-dependent TNL-mediated
441 resistance responses are activated when *BIR1* is overexpressed. We next found that the
442 expression of the PTI-markers *FRK1* and *RBOHD* remained elevated in DEX-treated *eds1-2*
443 BIR1 plants compared to non-treated controls (Figure 6d). *WRKY29* showed a tendency, albeit
444 not significant, to be up-regulated in these plants (Figure 6d). Thus, our data indicated that the
445 lack of *EDS1* attenuates the morphological phenotypes caused by *BIR1* overexpression, but has
446 no obvious effects on PTI gene expression. DEX-inducible expression of *BIR1* in *pad4-1* BIR1
447 mutant plants produced growth defects similar to those in BIR1 L9 plants, albeit yellowing was

448 less severe, indicating that mutations in *PAD4* were unable to rescue the *BIR1* overexpression
449 phenotypes (Figure 6b,c, S7a). Interestingly, the PTI-components *FRK1*, *WRKY29* and *RBOHD*
450 showed no responsiveness to *BIR1* overexpression in DEX-treated *pad4-1* BIR1 plants, which
451 suggests that PTI gene activation in these plants requires *PAD4* (Figure 6e). In summary, the
452 genetic elimination of *EDS1* mitigates the phenotypes caused by overexpression of *BIR1*,
453 whereas induction of PTI gene expression in *BIR1* overexpressing plants seems to depend on
454 *PAD4*.

455

456 3.5 Phenotypes of *BIR1* overexpressing lines are unrelated to SA signaling 457 pathways

458 Previously, high levels of SA were found to be partly responsible for *bir1-1* phenotypes (Gao
459 *et al.*, 2009). Here we tested the contribution of SA to the *BIR1* overexpression phenotypes.
460 First, we used Arabidopsis deficient in the *SALICYLIC ACID INDUCTION DEFICIENT 2*
461 (*SID2*)/ *ISOCHORISMATE SYNTHASE 1* (*ICS1*) and *EDS5* genes, which encode key SA
462 biosynthetic enzymes (Huang *et al.*, 2020), to infer their effects on the cell death phenotypes.
463 DEX-inducible BIR1-mCherry transgenic plants were generated in the *sid2-2* and *eds5-3* (*eds5*
464 is allelic to *sid1*) mutants, which contain low levels of SA (Nawrath *et al.*, 2002). The resulting
465 *eds5-3* BIR1 plants accumulated BIR1-mCherry protein like the BIR1 L9 control, whereas *sid2-*
466 *2* BIR1 produced less protein after 7 days of DEX applications (Figure 7a). Nevertheless, *sid2-*
467 *2* BIR1 and *eds5-3* BIR1 plants exhibited severe morphological phenotypes similar to those
468 observed in BIR1 L9 plants, and also accumulated high levels of *BIR1* transcripts after 12 days
469 of DEX treatment (Figure 7b, S7a). Thus, the *BIR1* overexpression phenotypes were likely
470 unrelated to SA levels.

471 Interestingly, RT-qPCR revealed that transcripts of the canonical SA-related defense marker
472 gene *PR1* were highly abundant in *BIR1* overexpressing *sid2-2* BIR1 *eds5-3* BIR1 plants
473 compared to mock-treated controls (Figure 7d). The induction of *PR1* transcripts was also
474 significant in SA-deficient, DEX-treated *sid2-2* BIR1 plants, but much less than in DEX-treated
475 BIR1 L9 plants or *eds5-3* BIR1 plants (Figure 7d). Thus, our finding suggests that SA-
476 independent mechanisms are also important for *PR1* expression in *BIR1* overexpressing plants.
477 PR1 gene expression was also up-regulated in DEX-treated *sobir1-12* BIR1 and *bak1-5* BIR1
478 plants, irrespective of their different morphological phenotypes (Figure 7d). During immunity,
479 *EDS1* and *PAD4* regulate SA-related defense gene expression and pathogen resistance through

480 ICS1-generated SA-dependent and SA-independent mechanisms (Tsuda *et al.*, 2013; Cui *et al.*,
481 2017). In our study, *PR1* expression was strongly enhanced in *eds1-2* BIR1 plants, but not in
482 *pad4-1* BIR1 plants, indicating that *PAD4*, but not *EDS1*, was required for *PR1* expression in
483 *BIR1* overexpressing plants (Jirage *et al.*, 1999) (Figure 7d). Together, our data propose that
484 the sustained expression of *BIR1* activates both SA-dependent and SA-independent
485 mechanisms of *PR1* induction whose contribution to *PR1* levels may differ between mutants.

486

487 3.6 Expression of phytohormone defense markers genes in compromised-defense 488 mutants overexpressing *BIR1*

489 RNA seq data indicated a significant transcriptional reprogramming of genes involved in
490 phytohormone metabolism and signaling in plants overexpressing *BIR1*. We determine the
491 expression of several well-characterized phytohormone-related marker genes in the above
492 Arabidopsis mutants defective in immune responses to infer the impact of plant hormone
493 signaling on the defects observed in *BIR1* overexpressing plants. Transcript levels of jasmonic
494 acid (JA)-responsive *PLANT DEFENSIN 1.2* (*PDF1.2*), ethylene ET- and JA-responsive *PR4*
495 as well as genes encoding the cytochrome P450 enzymes CYP71B15 (*PAD3*) and CYP79B2
496 involved in camalexin (CA)-biosynthesis and CA-mediated plant defense were analyzed by
497 RT-qPCR. None of these genes were affected by DEX in WT Arabidopsis plants.

498 Transcription of the *PDF1.2* gene was significantly up-regulated in all mutants tested, albeit to
499 varying degrees (Figure 8a). Compared to other *BIR1* overexpressing mutants, *PDF1.2*
500 transcripts were lower in *bak1-5* mutants, suggesting a role for *BAK1* in the regulation of JA-
501 signaling in *BIR1* overexpressing plants, as previously reported for JA-dependent resistance
502 against wounding or herbivory attacks (Figure 8a) (Yang *et al.*, 2011; Tungadi *et al.*, 2021).
503 *EDS1* and, to a lesser extent, *PAD4* act as repressors of JA/ET defense signaling (Brodersen *et*
504 *al.*, 2006). Consistently, we found that induction of *PDF1.2* was strong in *eds1-2* BIR1 mutants,
505 but weak, albeit significant, in *pad4-1* BIR1 plants (Figure 8a). The ET/JA marker *PR4* gene
506 was poorly activated in all *BIR1* overexpressing mutants tested, except in the SA-defective *sid2-*
507 *2* and *eds5-3* mutants, suggesting that the mutually antagonistic crosstalk between SA and
508 ET/JA pathways is unaffected by *BIR1* overexpression (Stroud *et al.*, 2022) (Figure 8b). The
509 expression of CA-related *PAD3* and *CYP79B2* genes was up-regulated, albeit to variable
510 extents, in all defense-compromised mutants tested upon *BIR1* overexpression, except *PAD4*-
511 dependent *PAD3* which, as predicted, remained as the non-treated controls in *pad4-1* mutants

512 (Zhou *et al.*, 1999) (Figure 8c). Interestingly, the transcriptional activation of genes encoding
513 markers in the JA, ET and CA pathways was particularly strong in DEX-treated *eds1-2* mutants,
514 which display partially rescued phenotypes, but weak in *pad4-1* mutants, which display typical
515 *BIR1* overexpression phenotypes. In summary, qRT-PCR analyses of canonical marker genes
516 suggest that the cell death-like morphological phenotypes observed in *BIR1* overexpressing
517 plants were not necessarily linked to the activation/inhibition of hormone defense signaling
518 pathways.

519

520 **4 DISCUSSION**

521 Plants respond to microbes and viruses by enhancing the expression of multiple genes that
522 function as regulators or executors of defense programs (Nishad *et al.*, 2020). Among them,
523 *BIR1* was shown to be transcriptionally up-regulated during bacterial and oomycete infections,
524 and also during viral infections in a SA-dependent manner (Gao *et al.*, 2009; Guzman-Benito
525 *et al.*, 2019). The observation that *bir1-1* mutants have increased resistance to the virulent
526 oomycete *Hyaloperonospora parasitica* Noco2 and to the RNA virus *Tobacco rattle virus*
527 (TRV) suggests an active role of *BIR1* in plant immunity (Gao *et al.*, 2009; Guzman-Benito *et*
528 *al.*, 2019). Previously we found that overexpression of *BIR1* in Arabidopsis using two
529 independent expression system, a viral vector or a transgenic inducible system, caused
530 senescence and cell death-like phenotypes. Intriguingly, these phenotypes were similar to those
531 observed under *BIR1* depletion in knockout plants, which suggest that defects in *BIR1*
532 regulation compromise the correct functioning of this gene. In order to investigate the genetic
533 components responsible for *BIR1* overexpressing phenotypes, we used a DEX-inducible system
534 to express a mCherry-tagged *BIR1* transgene in different Arabidopsis mutants defective in key
535 regulators of PTI and ETI signal transduction pathways. The resulting transgenic plants from
536 different genotypes accumulated BIR1-mCherry protein at comparable levels upon DEX
537 treatment, indicating similar induction efficiency in our experimental setting. Furthermore,
538 *BIR1* is triggered in the absence of immune elicitors or effectors that could otherwise initiate
539 undesirable localized and systemic defense responses in the plant.

540 We found that the cell death-type morphological phenotypes observed upon *BIR1*
541 overexpression was accompanied by the inappropriate overexpression of genes encoding
542 receptors and co-receptors with key functions in the perception of ligands/effectors and in the
543 regulation of defense signal transduction. The up-regulation of genes encoding TNL-resistance

544 proteins, but not CNLs, is an important feature linked to BIR1 overexpression. TNL-based
545 immunity is mediated by two distinct signaling modules, *EDS1*/*SAG101*/*NRG1* and
546 *EDS1*/*PAD4*/*ADR1* (Sun *et al.*, 2021). Here, we provide genetic evidence that the *BIR1*
547 overexpression morphological phenotypes are partially dependent on *EDS1*, but not on *PAD4*.
548 We propose that *EDS1*, perhaps in concert with *SAG101*, triggers cell death-like phenotypes
549 upon TNL activation in *BIR1* overexpressing plants (Figure 8d). How TNL receptors are
550 activated when *BIR1* is overexpressed is a question to resolve. A current model postulates that
551 loss of *BIR1* function leads to the activation of hypothetical guarding R proteins, which further
552 feed *PAD4*- and *SOBIR1*-dependent resistance pathways (Gao *et al.*, 2009). Our results are
553 coherent with BIR1 or a yet unknown BIR1/SERK complex being guarded by one or several
554 *EDS1*-dependent TNL proteins. Therefore, overexpression of *BIR1* may promote TNL-
555 mediated resistance pathways that require *EDS1* when no effectors or elicitors are present.

556 In addition to *EDS1*, we demonstrated that *SOBIR1* is necessary for *BIR1* overexpression
557 phenotypes. The role of *SOBIR1* in the *BIR1* pathway is unclear. Although extensive
558 investigation is required, S*OBIR1* may function as a specific co-regulator of the *EDS1*-
559 dependent responses triggered by *BIR1* overexpression, as part of the same signaling pathway
560 (Figure 8d). This idea is inspired by a recent work showing that the cell-surface RLP23 receptor
561 uses SOBIR1 to form a supramolecular complex with a EDS1/PAD4/ADR1 node in a ligand-
562 independent manner to mediate defense signaling cascades that are common to both surface
563 PRR (PTI) and NLR (ETI) receptors (Pruitt *et al.*, 2021b).

564 The TNL protein CSA1 senses perturbances of BIR3, BAK1 or BIR3/BAK1 complexes leading
565 to ETI-type autoimmune responses (Schulze *et al.*, 2022). *CSA1* did not show responsiveness
566 to *BIR1* overexpression in our assay, but it has been shown to interact with BIR1 (Schulze *et*
567 *al.*, 2022). It will be interesting to see if CSA1 also guards BIR1 integrity, perhaps in
568 cooperation with SOBIR1 and/or other SERKs (Figure 8d). Finally, phenotypes linked to *BIR1*
569 overexpression were apparently unaffected by the *bak1-5* mutation, which suggests that other
570 SERK family members can compensate for the loss of *BAK1* in PTI/ETI signaling.

571 We observed that the upregulation of *FRK1*, *WRKY29* and *RBOHD* due to *BIR1* overexpression
572 was compromised by mutations in *SOBIR1* and *PAD4,* but it was independent of *EDS1*. Since
573 *EDS1*, *PAD4* and *SOBIR1* are important for both cell surface PRR receptor- and TNL-mediated
574 signaling and resistance (Pruitt *et al.*, 2021b; Tian *et al.*, 2021), we will need additional
575 experimentation to establish if changes in PTI gene expression involve PTI-dependent
576 pathways, TNL activation or other unknown mechanisms yet to be determined. Our study also

577 reveals significant alterations in plant hormone gene expression caused by *BIR1*
578 overexpression. Interestingly, genes related to the plant hormones ET, JA, CA, and SA, which
579 play a central role in regulating immune responses, remained up-regulated in *eds1-2* BIR1 and
580 *sobir1-12* BIR1 backgrounds, in which phenotypes were partially rescued. This suggests that i)
581 regulation of hormone homeostasis does not require *SOBIR1*- and/or *EDS1*-mediated signaling
582 pathways, and that ii) the hormonal imbalance in BIR1 overexpressing plants has little, if any,
583 influence on the phenotypes.

584 The Arabidopsis heterotrimeric G protein AGB1 (SOBIR2) is a common signaling component
585 of PTI mediated by different RLK-PRRs, and functions in parallel with PAD4 downstream of
586 SOBIR1 to regulate cell death and pathogen resistance in *bir1-1* Arabidopsis mutants (Liu *et*
587 *al.*, 2013; Liang *et al.*, 2016). Similarly, Gγ-proteins AGG1/AGG2 have been described as
588 positive regulators of cell death and constitutive defense phenotypes in *bir1-1* mutants (Liu *et*
589 *al.*, 2013). *AGB1* and *AGG2* were up-regulated in *BIR1* overexpressing plants. These findings
590 bring up the idea that AGB1 and AGG1/2 could also function downstream of BIR1 to regulate
591 *EDS1*-mediated cell death when BIR1 integrity is disrupted. Equally important, the *BIR1*-
592 responsive GPA1 and XLG, in association with Gβγ modules, also have crucial roles in multiple
593 growth and developmental processes (Wang *et al.*, 2023). Thus, it is conceivable that
594 overactivation of these heterotrimeric G proteins due to the overexpression of *BIR1* may cause
595 indirect effects on plant development. Further studies are needed to test these plausible
596 hypotheses and their applicability to other plant species. In addition, identification of *BIR1*
597 interactors shall increase our understanding of the underlying mechanisms and components of
598 the *BIR1*-mediated regulation of immunity.

599 An interesting topic in this work is whether DEX treatment may be synergistically responsible
600 for the morphological phenotypes observed upon *BIR1* overexpression in the inducible system.
601 However, we find this possibility unconvincing. Although DEX may cause moderate plant
602 growth retardation in an age-dependent manner in our system, cell death/senescence
603 phenotypes were observed in none of the DEX-treated WT and mutant plants (without the
604 BIR1-mCherry cassette) or in transgenic plants expressing a mCherry-coding construct. In
605 addition, the cell death phenotypes described using the DEX-inducible system were similar to
606 those reported in WT Arabidopsis plants infected with a viral vector that overexpressed *BIR1*
607 fused to a HA protein tag. In these plants, phenotypes were normally stronger in infected tissue
608 accumulating high levels of HA-tagged BIR1 (Guzman-Benito *et al.*, 2019). Thus, it is unlikely
609 that the severe phenotypes observed in BIR1 L9 plants were an artifact caused by either DEX

610 treatment or mCherry overexpression, or by a synergistic interaction between DEX, *BIR1*
611 overexpression and tagged proteins (Guzman-Benito *et al.*, 2019). Because overexpression of
612 BIR1-mCherry has the same phenotypical outputs as HA-tagged BIR1 (Guzman-Benito *et al.*,
613 2019), and HA-tagging of *BIR1* produces a functional protein that is able to fully complement
614 *bir1-1* autoimmunity in Arabidopsis (Gao *et al.*, 2009), we suspect that the mCherry-tagging
615 does not compromise *BIR1* function in our transgenic setup. In summary, even though some
616 adverse effects due to long DEX treatments cannot be fully discarded in our experimental
617 system, specific effects linked to *BIR1* overexpression could be distinguished from other
618 potential combinatorial effects resulting from expressing an mCherry-tagged version of *BIR1*
619 in an activated glucocorticoid-inducible background (Kang *et al.*, 1999).

620 In conclusion, we investigated the implications of *BIR1* homeostasis on the immune response
621 in Arabidopsis. Overexpression of *BIR1* results in cell death phenotypes that resemble the
622 previously reported in loss-of-function *bir1-1* mutants. Furthermore, *BIR1* overexpression led
623 to massive transcriptomic changes affecting multiple defense-related genes. We show that both
624 *EDS1* and *SOBIR1* are necessary for the cell death phenotypes observed in *BIR1* overexpressing
625 plants, while *PAD4* and *BAK1* are not. We hypothesize that BIR1, previously thought to
626 represent a negative regulator of plant immunity, is a guarded protein surveilled by unknown
627 TNLs, with SOBIR1 working alongside EDS1 to transduce signals downstream of the TNLs
628 (Figure 8d).

629

630 **ACKNOWLEDGEMENTS**

631 We thank members of the César Llave lab and to my colleagues Manfred Heinlein (Institut de
632 Biologie Moléculaire des Plantes, CNRS, Strasbourg, France), Rosa Lozano-Durán, Birgit
633 Kemmerling, Thorsten Nürnberger (Center of Plant Molecular Biology, University of
634 Tübingen, Tübingen, Germany) and Francisco Tenllado (Centro de Investigaciones Biológicas
635 Margarita Salas, CSIC, Madrid, Spain) for helpful discussions. We thank Monica Fontenla for
636 technical support.

637

638 **REFERENCES**

639 **Albert I, Zhang L, Bemm H, Nurnberger T. 2019.** Structure-Function Analysis of Immune
640 Receptor AtRLP23 with Its Ligand nlp20 and Coreceptors AtSOBIR1 and AtBAK1. *Mol*
641 *Plant Microbe Interact* **32**(8): 1038-1046.
642 **Belkhadir Y, Jaillais Y, Epple P, Balsemao-Pires E, Dangl JL, Chory J. 2012.**
643 Brassinosteroids modulate the efficiency of plant immune responses to microbe-associated
644 molecular patterns. *Proc Natl Acad Sci U S A* **109**(1): 297-302.
645 **Bi G, Zhou Z, Wang W, Li L, Rao S, Wu Y, Zhang X, Menke FLH, Chen S, Zhou JM.**
646 **2018.** Receptor-Like Cytoplasmic Kinases Directly Link Diverse Pattern Recognition
647 Receptors to the Activation of Mitogen-Activated Protein Kinase Cascades in Arabidopsis.
648 *Plant Cell* **30**(7): 1543-1561.
649 **Boudsocq M, Willmann MR, McCormack M, Lee H, Shan L, He P, Bush J, Cheng SH,**
650 **Sheen J. 2010.** Differential innate immune signalling via Ca(2+) sensor protein kinases.
651 *Nature* **464**(7287): 418-422.
652 **Boutrot F, Zipfel C. 2017.** Function, Discovery, and Exploitation of Plant Pattern Recognition
653 Receptors for Broad-Spectrum Disease Resistance. *Annu Rev Phytopathol* **55**: 257-286.
654 **Boyes DC, Zayed AM, Ascenzi R, McCaskill AJ, Hoffman NE, Davis KR, Gorlach J. 2001.**
655 Growth stage-based phenotypic analysis of Arabidopsis: a model for high throughput
656 functional genomics in plants. *Plant Cell* **13**(7): 1499-1510.
657 **Brodersen P, Petersen M, Bjorn Nielsen H, Zhu S, Newman MA, Shokat KM, Rietz S,**
658 **Parker J, Mundy J. 2006.** Arabidopsis MAP kinase 4 regulates salicylic acid- and jasmonic
659 acid/ethylene-dependent responses via EDS1 and PAD4. *Plant J* **47**(4): 532-546.
660 **Brutus A, Sicilia F, Macone A, Cervone F, De Lorenzo G. 2010.** A domain swap approach
661 reveals a role of the plant wall-associated kinase 1 (WAK1) as a receptor of
662 oligogalacturonides. *Proc Natl Acad Sci U S A* **107**(20): 9452-9457.
663 **Cao Y, Liang Y, Tanaka K, Nguyen CT, Jedrzejczak RP, Joachimiak A, Stacey G. 2014.**
664 The kinase LYK5 is a major chitin receptor in Arabidopsis and forms a chitin-induced
665 complex with related kinase CERK1. *Elife* **3**.
666 **Castro B, Citterico M, Kimura S, Stevens DM, Wrzaczek M, Coaker G. 2021.** Stress-
667 induced reactive oxygen species compartmentalization, perception and signalling. *Nat*
668 *Plants* **7**(4): 403-412.
669 **Chen Z. 2001.** A superfamily of proteins with novel cysteine-rich repeats. *Plant Physiol* **126**(2):
670 473-476.
671 **Clough SJ, Bent AF. 1998.** Floral dip: a simplified method for Agrobacterium-mediated
672 transformation of Arabidopsis thaliana. *Plant J* **16**(6): 735-743.

673 **Couto D, Zipfel C. 2016.** Regulation of pattern recognition receptor signalling in plants. *Nat*
674 *Rev Immunol* **16**(9): 537-552.
675 **Cui H, Gobbato E, Kracher B, Qiu J, Bautor J, Parker JE. 2017.** A core function of EDS1
676 with PAD4 is to protect the salicylic acid defense sector in Arabidopsis immunity. *New*
677 *Phytol* **213**(4): 1802-1817.
678 **Dominguez-Ferreras A, Kiss-Papp M, Jehle AK, Felix G, Chinchilla D. 2015.** An Overdose
679 of the Arabidopsis Coreceptor BRASSINOSTEROID INSENSITIVE1-ASSOCIATED
680 RECEPTOR KINASE1 or Its Ectodomain Causes Autoimmunity in a SUPPRESSOR OF
681 BIR1-1-Dependent Manner. *Plant Physiol* **168**(3): 1106-1121.
682 **Faulkner C, Petutschnig E, Benitez-Alfonso Y, Beck M, Robatzek S, Lipka V, Maule AJ.**
683 **2013.** LYM2-dependent chitin perception limits molecular flux via plasmodesmata. *Proc*
684 *Natl Acad Sci U S A* **110**(22): 9166-9170.
685 **Fernandez-Calvino L, Guzman-Benito I, Del Toro FJ, Donaire L, Castro-Sanz AB, Ruiz-**
686 **Ferrer V, Llave C. 2016.** Activation of senescence-associated Dark-inducible (DIN) genes
687 during infection contributes to enhanced susceptibility to plant viruses. *Mol Plant Pathol*
688 **17**(1): 3-15.
689 **Freh M, Gao JL, Petersen M, Panstruga R. 2022.** Plant autoimmunity-fresh insights into an
690 old phenomenon. *Plant Physiology* **188**(3): 1419-1434.
691 **Gao M, Wang X, Wang D, Xu F, Ding X, Zhang Z, Bi D, Cheng YT, Chen S, Li X, et al.**
692 **2009.** Regulation of cell death and innate immunity by two receptor-like kinases in
693 Arabidopsis. *Cell Host Microbe* **6**(1): 34-44.
694 **Gust AA, Pruitt R, Nurnberger T. 2017.** Sensing Danger: Key to Activating Plant Immunity.
695 *Trends Plant Sci* **22**(9): 779-791.
696 **Guzman-Benito I, Donaire L, Amorim-Silva V, Vallarino JG, Esteban A, Wierzbicki AT,**
697 **Ruiz-Ferrer V, Llave C. 2019.** The immune repressor BIR1 contributes to antiviral defense
698 and undergoes transcriptional and post-transcriptional regulation during viral infections.
699 *New Phytol* **224**(1): 421-438.
700 **Halter T, Imkampe J, Mazzotta S, Wierzba M, Postel S, Bucherl C, Kiefer C, Stahl M,**
701 **Chinchilla D, Wang X, et al. 2014.** The leucine-rich repeat receptor kinase BIR2 is a
702 negative regulator of BAK1 in plant immunity. *Curr Biol* **24**(2): 134-143.
703 **He ZH, Fujiki M, Kohorn BD. 1996.** A cell wall-associated, receptor-like protein kinase. *J*
704 *Biol Chem* **271**(33): 19789-19793.
705 **Hohmann U, Lau K, Hothorn M. 2017.** The Structural Basis of Ligand Perception and Signal
706 Activation by Receptor Kinases. *Annu Rev Plant Biol* **68**: 109-137.

Hou S, Liu D, Huang S, Luo D, Liu Z, Xiang Q, Wang P, Mu R, Han Z, Chen S, et al. 2021. The Arabidopsis MIK2 receptor elicits immunity by sensing a conserved signature from phytocytokines and microbes. *Nat Commun* **12**(1): 5494.

Huang W, Wang Y, Li X, Zhang Y. 2020. Biosynthesis and Regulation of Salicylic Acid and N-Hydroxypipecolic Acid in Plant Immunity. *Mol Plant* **13**(1): 31-41.

Imkampe J, Halter T, Huang S, Schulze S, Mazzotta S, Schmidt N, Manstretta R, Postel S, Wierzba M, Yang Y, et al. 2017. The Arabidopsis Leucine-Rich Repeat Receptor Kinase BIR3 Negatively Regulates BAK1 Receptor Complex Formation and Stabilizes BAK1. *Plant Cell* **29**(9): 2285-2303.

Jirage D, Tootle TL, Reuber TL, Frost LN, Feys BJ, Parker JE, Ausubel FM, Glazebrook J. 1999. Arabidopsis thaliana PAD4 encodes a lipase-like gene that is important for salicylic acid signaling. *Proc Natl Acad Sci U S A* **96**(23): 13583-13588.

Jubic LM, Saile S, Furzer OJ, El Kasmi F, Dangl JL. 2019. Help wanted: helper NLRs and plant immune responses. *Curr Opin Plant Biol* **50**: 82-94.

Kadota Y, Sklenar J, Derbyshire P, Stransfeld L, Asai S, Ntoukakis V, Jones JD, Shirasu K, Menke F, Jones A, et al. 2014. Direct regulation of the NADPH oxidase RBOHD by the PRR-associated kinase BIK1 during plant immunity. *Mol Cell* **54**(1): 43-55.

Kang HG, Fang YW, Singh KB. 1999. A glucocorticoid-inducible transcription system causes severe growth defects in

and induces defense-related genes. *Plant Journal* **20**(1): 127-133.

Kato H, Nemoto K, Shimizu M, Abe A, Asai S, Ishihama N, Matsuoka S, Daimon T, Ojika M, Kawakita K, et al. 2022. Recognition of pathogen-derived sphingolipids in Arabidopsis. *Science* **376**(6595): 857-860.

Korner CJ, Klauser D, Niehl A, Dominguez-Ferreras A, Chinchilla D, Boller T, Heinlein M, Hann DR. 2013. The immunity regulator BAK1 contributes to resistance against diverse RNA viruses. *Mol Plant Microbe Interact* **26**(11): 1271-1280.

Krol E, Mentzel T, Chinchilla D, Boller T, Felix G, Kemmerling B, Postel S, Arents M, Jeworutzki E, Al-Rasheid KA, et al. 2010. Perception of the Arabidopsis danger signal peptide 1 involves the pattern recognition receptor AtPEPR1 and its close homologue AtPEPR2. *J Biol Chem* **285**(18): 13471-13479.

Li L, Li M, Yu L, Zhou Z, Liang X, Liu Z, Cai G, Gao L, Zhang X, Wang Y, et al. 2014. The FLS2-associated kinase BIK1 directly phosphorylates the NADPH oxidase RbohD to control plant immunity. *Cell Host Microbe* **15**(3): 329-338.

740 **Li P, Lu YJ, Chen H, Day B. 2020.** The Lifecycle of the Plant Immune System. *CRC Crit Rev*
741 *Plant Sci* **39**(1): 72-100.
742 **Liang X, Ding P, Lian K, Wang J, Ma M, Li L, Li L, Li M, Zhang X, Chen S, et al. 2016.**
743 Arabidopsis heterotrimeric G proteins regulate immunity by directly coupling to the FLS2
744 receptor. *Elife* **5**: e13568.
745 **Liang X, Zhou JM. 2018.** Receptor-Like Cytoplasmic Kinases: Central Players in Plant
746 Receptor Kinase-Mediated Signaling. *Annu Rev Plant Biol* **69**: 267-299.
747 **Liu J, Ding P, Sun T, Nitta Y, Dong O, Huang X, Yang W, Li X, Botella JR, Zhang Y.**
748 **2013.** Heterotrimeric G proteins serve as a converging point in plant defense signaling
749 activated by multiple receptor-like kinases. *Plant Physiol* **161**(4): 2146-2158.
750 **Liu Y, Huang X, Li M, He P, Zhang Y. 2016.** Loss-of-function of Arabidopsis receptor-like
751 kinase BIR1 activates cell death and defense responses mediated by BAK1 and SOBIR1.
752 *New Phytol* **212**(3): 637-645.
753 **Luo X, Wu W, Liang Y, Xu N, Wang Z, Zou H, Liu J. 2020.** Tyrosine phosphorylation of
754 the lectin receptor-like kinase LORE regulates plant immunity. *Embo J* **39**(4): e102856.
755 **Lv Y, Yang N, Wu J, Liu Z, Pan L, Lv S, Wang G. 2016.** New insights into receptor-like
756 protein functions in Arabidopsis. *Plant Signal Behav* **11**(7): e1197469.
757 **McNellis TW, Mudgett MB, Li K, Aoyama T, Horvath D, Chua NH, Staskawicz BJ. 1998.**
758 Glucocorticoid-inducible expression of a bacterial avirulence gene in transgenic Arabidopsis
759 induces hypersensitive cell death. *Plant J* **14**(2): 247-257.
760 **Mithoe SC, Menke FL. 2018.** Regulation of pattern recognition receptor signalling by
761 phosphorylation and ubiquitination. *Curr Opin Plant Biol* **45**(Pt A): 162-170.
762 **Nawrath C, Heck S, Parinthawong N, Metraux JP. 2002.** EDS5, an essential component of
763 salicylic acid-dependent signaling for disease resistance in Arabidopsis, is a member of the
764 MATE transporter family. *Plant Cell* **14**(1): 275-286.
765 **Ngou BPM, Ahn HK, Ding P, Jones JDG. 2021.** Mutual potentiation of plant immunity by
766 cell-surface and intracellular receptors. *Nature* **592**(7852): 110-115.
767 **Nishad R, Ahmed T, Rahman VJ, Kareem A. 2020.** Modulation of Plant Defense System in
768 Response to Microbial Interactions. *Front Microbiol* **11**: 1298.
769 **Ouwerkerk PB, de Kam RJ, Hoge JH, Meijer AH. 2001.** Glucocorticoid-inducible gene
770 expression in rice. *Planta* **213**(3): 370-378.
771 **Parker JE, Holub EB, Frost LN, Falk A, Gunn ND, Daniels MJ. 1996.** Characterization of
772 eds1, a mutation in Arabidopsis suppressing resistance to Peronospora parasitica specified
773 by several different RPP genes. *Plant Cell* **8**(11): 2033-2046.

774 **Pruitt RN, Gust AA, Nurnberger T. 2021a.** Plant immunity unified. *Nat Plants* **7**(4): 382-
775 383.
776 **Pruitt RN, Locci F, Wanke F, Zhang L, Saile SC, Joe A, Karelina D, Hua C, Frohlich K,**
777 **Wan WL, et al. 2021b.** The EDS1-PAD4-ADR1 node mediates Arabidopsis pattern-
778 triggered immunity. *Nature* **598**(7881): 495-499.
779 **Quezada EH, Garcia GX, Arthikala MK, Melappa G, Lara M, Nanjareddy K. 2019.**
780 Cysteine-Rich Receptor-Like Kinase Gene Family Identification in the Phaseolus Genome
781 and Comparative Analysis of Their Expression Profiles Specific to Mycorrhizal and
782 Rhizobial Symbiosis. *Genes (Basel)* **10**(1).
783 **Rao S, Zhou Z, Miao P, Bi G, Hu M, Wu Y, Feng F, Zhang X, Zhou JM. 2018.** Roles of
784 Receptor-Like Cytoplasmic Kinase VII Members in Pattern-Triggered Immune Signaling.
785 *Plant Physiol* **177**(4): 1679-1690.
786 **Rodriguez E, El Ghoul H, Mundy J, Petersen M. 2016.** Making sense of plant autoimmunity
787 and 'negative regulators'. *FEBS J* **283**(8): 1385-1391.
788 **Schulze S, Yu L, Hua C, Zhang L, Kolb D, Weber H, Ehinger A, Saile SC, Stahl M, Franz-**
789 **Wachtel M, et al. 2022.** The Arabidopsis TIR-NBS-LRR protein CSA1 guards BAK1-BIR3
790 homeostasis and mediates convergence of pattern- and effector-induced immune responses.
791 *Cell Host Microbe* **30**(12): 1717-1731 e1716.
792 **Schwessinger B, Roux M, Kadota Y, Ntoukakis V, Sklenar J, Jones A, Zipfel C. 2011.**
793 Phosphorylation-dependent differential regulation of plant growth, cell death, and innate
794 immunity by the regulatory receptor-like kinase BAK1. *PLoS Genet* **7**(4): e1002046.
795 **Smakowska-Luzan E, Mott GA, Parys K, Stegmann M, Howton TC, Layeghifard M,**
796 **Neuhold J, Lehner A, Kong J, Grunwald K, et al. 2018.** An extracellular network of
797 Arabidopsis leucine-rich repeat receptor kinases. *Nature* **553**(7688): 342-346.
798 **Stroud EA, Jayaraman J, Templeton MD, Rikkerink EHA. 2022.** Comparison of the
799 pathway structures influencing the temporal response of salicylate and jasmonate defence
800 hormones in Arabidopsis thaliana. *Front Plant Sci* **13**: 952301.
801 **Sun X, Lapin D, Feehan JM, Stolze SC, Kramer K, Dongus JA, Rzemieniewski J,**
802 **Blanvillain-Baufume S, Harzen A, Bautor J, et al. 2021.** Pathogen effector recognition-
803 dependent association of NRG1 with EDS1 and SAG101 in TNL receptor immunity. *Nat*
804 *Commun* **12**(1): 3335.
805 **Swiderski MR, Birker D, Jones JD. 2009.** The TIR domain of TIR-NB-LRR resistance
806 proteins is a signaling domain involved in cell death induction. *Mol Plant Microbe Interact*
807 **22**(2): 157-165.

808 **Tian H, Wu Z, Chen S, Ao K, Huang W, Yaghmaiean H, Sun T, Xu F, Zhang Y, Wang S,**
809 **et al. 2021.** Activation of TIR signalling boosts pattern-triggered immunity. *Nature*
810 **598**(7881): 500-503.
811 **Tsuda K, Mine A, Bethke G, Igarashi D, Botanga CJ, Tsuda Y, Glazebrook J, Sato M,**
812 **Katagiri F. 2013.** Dual regulation of gene expression mediated by extended MAPK
813 activation and salicylic acid contributes to robust innate immunity in Arabidopsis thaliana.
814 *PLoS Genet* **9**(12): e1004015.
815 **Tungadi T, Watt LG, Groen SC, Murphy AM, Du Z, Pate AE, Westwood JH, Fennell TG,**
816 **Powell G, Carr JP. 2021.** Infection of Arabidopsis by cucumber mosaic virus triggers
817 jasmonate-dependent resistance to aphids that relies partly on the pattern-triggered immunity
818 factor BAK1. *Mol Plant Pathol* **22**(9): 1082-1091.
819 **van Wersch S, Tian L, Hoy R, Li X. 2020.** Plant NLRs: The Whistleblowers of Plant
820 Immunity. *Plant Commun* **1**(1): 100016.
821 **Wan J, Tanaka K, Zhang XC, Son GH, Brechenmacher L, Nguyen TH, Stacey G. 2012.**
822 LYK4, a lysin motif receptor-like kinase, is important for chitin signaling and plant innate
823 immunity in Arabidopsis. *Plant Physiol* **160**(1): 396-406.
824 **Wan WL, Zhang L, Pruitt R, Zaidem M, Brugman R, Ma X, Krol E, Perraki A, Kilian J,**
825 **Grossmann G, et al. 2019.** Comparing Arabidopsis receptor kinase and receptor protein-
826 mediated immune signaling reveals BIK1-dependent differences. *New Phytol* **221**(4): 2080-
827 2095.
828 **Wang G, Ellendorff U, Kemp B, Mansfield JW, Forsyth A, Mitchell K, Bastas K, Liu CM,**
829 **Woods-Tor A, Zipfel C, et al. 2008.** A genome-wide functional investigation into the roles
830 of receptor-like proteins in Arabidopsis. *Plant Physiol* **147**(2): 503-517.
831 **Wang J, Chai J. 2020.** Structural Insights into the Plant Immune Receptors PRRs and NLRs.
832 *Plant Physiol* **182**(4): 1566-1581.
833 **Wang Y, Zhang H, Wang P, Zhong H, Liu W, Zhang S, Xiong L, Wu Y, Xia Y. 2023.**
834 Arabidopsis EXTRA-LARGE G PROTEIN 1 (XLG1) functions together with XLG2 and
835 XLG3 in PAMP-triggered MAPK activation and immunity. *J Integr Plant Biol* **65**(3): 825-
836 837.
837 **Willmann R, Lajunen HM, Erbs G, Newman MA, Kolb D, Tsuda K, Katagiri F,**
838 **Fliegmann J, Bono JJ, Cullimore JV, et al. 2011.** Arabidopsis lysin-motif proteins LYM1
839 LYM3 CERK1 mediate bacterial peptidoglycan sensing and immunity to bacterial infection.
840 *Proc Natl Acad Sci U S A* **108**(49): 19824-19829.

841 **Withers J, Dong X. 2017.** Post-translational regulation of plant immunity. *Curr Opin Plant*
842 *Biol* **38**: 124-132.
843 **Wu Y, Gao Y, Zhan Y, Kui H, Liu H, Yan L, Kemmerling B, Zhou JM, He K, Li J. 2020.**
844 Loss of the common immune coreceptor BAK1 leads to NLR-dependent cell death. *Proc*
845 *Natl Acad Sci U S A* **117**(43): 27044-27053.
846 **Yang DH, Hettenhausen C, Baldwin IT, Wu J. 2011.** BAK1 regulates the accumulation of
847 jasmonic acid and the levels of trypsin proteinase inhibitors in Nicotiana attenuata's
848 responses to herbivory. *J Exp Bot* **62**(2): 641-652.
849 **Yeh YH, Chang YH, Huang PY, Huang JB, Zimmerli L. 2015.** Enhanced Arabidopsis
850 pattern-triggered immunity by overexpression of cysteine-rich receptor-like kinases. *Front*
851 *Plant Sci* **6**: 322.
852 **Yip Delormel T, Boudsocq M. 2019.** Properties and functions of calcium-dependent protein
853 kinases and their relatives in Arabidopsis thaliana. *New Phytol* **224**(2): 585-604.
854 **Yu TY, Sun MK, Liang LK. 2021.** Receptors in the Induction of the Plant Innate Immunity.
855 *Mol Plant Microbe Interact* **34**(6): 587-601.
856 **Yuan M, Cai B, Xin XF. 2023.** Plant immune receptor pathways as a united front against
857 pathogens. *PLoS Pathog* **19**(2): e1011106.
858 **Yuan M, Jiang Z, Bi G, Nomura K, Liu M, Wang Y, Cai B, Zhou JM, He SY, Xin XF.**
859 **2021a.** Pattern-recognition receptors are required for NLR-mediated plant immunity. *Nature*
860 **592**(7852): 105-109.
861 **Yuan M, Ngou BPM, Ding P, Xin XF. 2021b.** PTI-ETI crosstalk: an integrative view of plant
862 immunity. *Curr Opin Plant Biol* **62**: 102030.
863 **Zhang W, Fraiture M, Kolb D, Loffelhardt B, Desaki Y, Boutrot FF, Tor M, Zipfel C,**
864 **Gust AA, Brunner F. 2013.** Arabidopsis receptor-like protein30 and receptor-like kinase
865 suppressor of BIR1-1/EVERSHED mediate innate immunity to necrotrophic fungi. *Plant*
866 *Cell* **25**(10): 4227-4241.
867 **Zhong CL, Zhang C, Liu JZ. 2019.** Heterotrimeric G protein signaling in plant immunity. *J*
868 *Exp Bot* **70**(4): 1109-1118.
869 **Zhou JM, Zhang Y. 2020.** Plant Immunity: Danger Perception and Signaling. *Cell* **181**(5):
870 978-989.
871 **Zhou N, Tootle TL, Glazebrook J. 1999.** Arabidopsis PAD3, a gene required for camalexin
872 biosynthesis, encodes a putative cytochrome P450 monooxygenase. *Plant Cell* **11**(12): 2419-
873 2428.

874 **Zhou N, Tootle TL, Tsui F, Klessig DF, Glazebrook J. 1998.** PAD4 functions upstream from
875 salicylic acid to control defense responses in Arabidopsis. *Plant Cell* **10**(6): 1021-1030.

876

877 AUTHOR CONTRIBUTIONS

878 CL and IGB conceived and designed the study. CL, IGB, CR and IP performed expression
879 assays and transgenics. CL and IGB analyzed the data. CL wrote the article.

880

881 SUPPORTING INFORMATION

882 The following materials are available in the online version of this article.

883

884 **Figure S1.** Transcriptomic profiling of dexamethasone (DEX)-treated wild-type Col-0 plants.

885 **Figure S2.** Transcriptomic profiling of *BIR1* expressing transgenic lines.

886 **Figure S3.** Enrichment analysis of Kyoto Encyclopedia of Genes and Genomes (KEGG)
887 pathways using RNA-Seq data.

888 **Figure S4.** Differential expression of cell-surface pattern recognition receptors (PRR)-coding
889 genes in *BIR1* overexpressing plants.

890 **Figure S5.** Differential expression of calcium-dependent protein kinases (CPK)-coding genes
891 in *BIR1* overexpressing plants.

892 **Figure S6.** Differential expression of *HETEROTRIMERIC G PROTEIN* genes in *BIR1*
893 overexpressing plants.

894 **Figure S7.** Morphological and growth defects in independent dexamethasone (DEX)-treated
895 *BIR1* overexpressing plants of different immune mutant genetic backgrounds.

896 **Figure S8.** Morphological phenotypes of dexamethasone (DEX)-treated immune mutant
897 genetic backgrounds and mCherry transgenic plants.

898

899 **Table S1**. List of primers

900 **Table S2**. List of expressed genes.

901 **Table S3**. List of differentially expressed genes (DEG. padjust value < 0.05).

902 **Table S4**. List of differentially expressed genes (DEG. |Log_2fold change > 1| padjust value <
903 0.01).

904 **Table S5**. Enrichment analysis of Gene Ontology (GO) terms.

905 **Table S6**. Kyoto Encyclopedia of Genes and Genomes (KEGG) pathway enrichment analysis.
906 **Table S7**. List of differentially expressed genes (DEG. padjust value < 0.05) within functional
907 categories.

908 **Table S8**. Statistical analysis of enrichment of functional gene groups in plants overexpressing
909 BIR1 after 12 days of DEX treatment relative to non-expressing controls using Two-tailed
910 Fisher's exact tests.

911

912 ## FUNDING

913 This work was supported by National Research grants RTI2018-096979-B-I00 and PID2021
914 127982NB-I00 to CL from Ministerio de Ciencia e Innovación (Spain) and UE-FEDER, and
915 grant iLINKA20415 to CL from CSIC (Spain).

916

917 ## Data availability

918 The data supporting this study's findings are available from the corresponding author upon
919 reasonable request.

920

921

922 ## Figure legends

923 **Figure 1**

924 Transcriptional reprogramming associated with *BIR1* induction in Arabidopsis. **(a)** Morphology
925 of representative dexamethasone (DEX)-inducible BIR1-mCherry transgenic Arabidopsis
926 plants from line 9 (L9). Photographs were taken after 10-12 days of 30 μM DEX. Mock-treated
927 wild-type (WT) Arabidopsis were used as controls. DEX treatments started at the Boyes growth
928 stage 1.7. Cell-death phenotypes in Arabidopsis DEX-treated BIR1 L9 plants were similar to
929 those observed when BIR1-HA was expressed via TRV infection (TRV-BIR1). **(b)** Western
930 blot using anti-mCherry antibody shows the relative accumulation of BIR1-mCherry protein
931 after 4 and 12 days of DEX treatments in BIR1 L9 plants. **(c)** Number of up-or down-regulated
932 transcripts, with a $|\log_2 \text{(Fold-Change)}| \geq 1$ and adjusted *p*-value ≤ 0.01, in each pairwise
933 comparison is indicated. **(d)** Principal component analysis (PCA) of RNA-Seq data. The PCA
934 was performed using normalized RNA-Seq data of differentially expressed genes (DEGs) under
935 each condition: Mock-treated WT (Mock-WT), Mock-treated BIR1 L9 (Mock-L9), DEX-
936 treated WT (DEX-WT), DEX-treated BIR1 L9 (DEX-L9). Samples were collected after 4 and
937 12 days of DEX treatment as indicated. Each biological replicate is represented in the score
938 plot. The variance explained by each component (%) is given in parentheses. The sample
939 (DeL9_12b) with differential expression within the DEX-treated L9 group is indicated with an
940 arrow. **(e)** Relative expression of the BIR1-coding gene based on the number of Fragments Per
941 Kilobase of transcript sequence per Millions of base-pairs sequenced (FPKM) (top). Significant
942 differences between DEX- and mock-treated samples were analyzed using two-way ANOVA
943 followed by Sidak´s multiple comparison test; ***, adjusted *p*-value < 0.001. **(f)** Scatterplot of
944 selected gene ontology (GO) terms of DEGs. GO terms between WT and BIR1 L9 plants after
945 12 days of DEX-treatment (DeL9_ vs DeWT_) are shown. Dot size represents the count of
946 different genes and the color indicates significance of the term enrichment. GO terms with
947 adjusted *p*-value < 0.05 are significantly enriched. The kinase term (indicated by an arrow) was
948 exclusively assigned to BIR1 L9 plants.

949

950 **Figure 2**

951 Differential expression of cysteine-rich receptor-like kinase (CRK)-coding genes in *BIR1*
952 overexpressing plants. **(a)** Expression of selected BIR1-responsive differentially expressed
953 genes (DEGs) based on fold-change values ($\log_2$ DeL9_12/DeWT_12 and $\log_2$

954 DeL9_12/MoL9_12 as indicated) was confirmed by RT-qPCR. Values from biologically
955 independent samples were normalized to the *CBP20* internal control, and related to untreated
956 (DEX-) plants, set to a value of 1. Data are mean ± SD analyzed by Mann-Whitney test; *, p
957 <0.05. **(b)** Expression of CRK-coding differentially expressed genes based on $\log_2$ fold-change
958 in BIR1 overexpressing plants as indicated. (**c)** Relative expression levels of CRK-coding genes
959 represented by the number of Fragments Per Kilobase of transcript sequence per Millions of
960 base-pairs sequenced (FPKM) in each of the three independent samples per condition used for
961 RNA-Seq. Significant differences between dexamethasone (DEX)- and mock-treated samples
962 were analyzed using two-way ANOVA followed by Sidak´s multiple comparison test; ***,
963 adjusted p-value < 0.001, **< 0.01. Note that the expression levels of each individual replicate
964 within the DEX-treated BIR1 L9_12 group mirror the abundance of *BIR1* transcripts in each
965 replicate. Values from the DeL9_12b sample are indicated by an arrowhead.

966

967 **Figure 3**

968 Differential expression of receptor-like protein (RLP)-coding genes in *BIR1* overexpressing
969 plants. **(a)** Expression of differentially expressed RLP-coding genes based on $\log_2$ fold-change
970 as indicated. **(b)** Relative expression levels of RLP-coding genes represented by the number of
971 Fragments Per Kilobase of transcript sequence per Millions of base-pairs sequenced (FPKM)
972 in each of the three independent samples per condition used for RNA-Seq. Significant
973 differences between dexamethasone (DEX)- and mock-treated samples were analyzed using
974 two-way ANOVA followed by Sidak´s multiple comparison test; ***, adjusted p-value < 0.001,
975 **< 0.01. Note that the expression levels of each individual replicate within the DEX-treated
976 BIR1 L9_12 group mirror the abundance of *BIR1* transcripts in each replicate. Values from the
977 DeL9_12b sample are indicated by an arrowhead.

978

979 **Figure 4**

980 *BIR1* overexpression leads to the transcriptional activation of pattern-triggered immunity (PTI)-
981 associated co-receptors and effector-triggered immunity (ETI) regulators. Relative expression
982 of selected genes encoding PTI/ETI-markers based on the number of Fragments Per Kilobase
983 of transcript sequence per Millions of base-pairs sequenced (FPKM) in each of the three
984 independent samples per condition used for RNA-Seq. Actin expression is shown as control.
985 Note that the expression levels of each individual replicate within the DEX-treated BIR1 L9_12

986 group mirror the abundance of *BIR1* transcripts in each replicate. DeL9_12b is indicated by a
987 red arrow. Significant differences between mock-treated and DEX-treated samples were
988 analyzed using two-way ANOVA followed by Sidak´s multiple comparison test; **, adjusted
989 *p*-value < 0.01, * < 0.05. Values from the DeL9_12b sample are indicated by an arrowhead.

990

991 **Figure 5**

992 Phenotypes caused by *BIR1* overexpression are partially rescued in *sobir1-12* mutants. **(a)**
993 Western blot analysis of BIR1-mCherry proteins in the dexamethasone (DEX)-inducible BIR1-
994 mCherry transgenic Arabidopsis lines wild-type (WT) BIR1 L9, *sobir1-12* BIR1 (L6) and *bak1-*
995 5 BIR1 (L10) treated with DEX for 7 days. Each sample is a pool of two plants, and two samples
996 per genotype are shown. Protein loading control by Ponceau S is shown. **(b)** Morphology of
997 representative WT BIR1 L9, *sobir1-12* BIR1 L6 and *bak1*-5 BIR1 L10 plants. Images from
998 independent transgenic lines are shown in **Figure S8**. **(c)** RT-qPCR analysis of *BIR1* transcripts
999 in WT BIR1 L9, *sobir1-12* BIR1 L6 and *bak1*-5 BIR1 L10 plants. **(d, e)** RT-qPCR analysis of
1000 PTI-markers *RBOHD*, *FRK1* or *WRKY29* in *sobir1-12* BIR1 L6 **(d)** and *bak1*-5 BIR1 L10 **(e)**
1001 plants. Photographs and samples for qRT-PCR were taken after 12 days of 30 µM DEX
1002 treatment. Measures were done in mock-treated (DEX-) versus DEX-treated (DEX+) using the
1003 same set of replicates from each genotype. Values from biologically independent samples were
1004 normalized to the *CBP20* internal control, and related to mock-treated plants, set to a value of
1005 1. Data are mean ± SD analyzed by Mann-Whitney test; *, *p* <0.05. Experiments were repeated
1006 at least twice with similar results.

1007

1008 **Figure 6**

1009 Phenotypes caused by *BIR1* overexpression are partially rescued in *eds1-2* mutants, but not in
1010 *pad4-1* mutants. **(a)** Western blot analysis of BIR1-mCherry proteins in the dexamethasone
1011 (DEX)-inducible BIR1-mCherry transgenic Arabidopsis lines wild-type (WT) BIR1 L9, *eds1-*
1012 *2* BIR1 L1b and *pad4-1* BIR1 L0 treated with DEX for 7 days. Each sample is a pool of two
1013 plants, and three samples per genotype are shown. Protein loading control by Ponceau S is
1014 shown. **(b)** Morphology of representative *eds1-2* BIR1 L1b and *pad4-1* BIR1 L0 plants. Images
1015 from independent transgenic lines are shown in Figure S8. **(c)** RT-qPCR analysis of *BIR1*
1016 transcripts in *eds1-2* BIR1 L1b and *pad4-1* BIR1 L0 mutant lines. **(d, e)** RT-qPCR analysis of
1017 PTI-markers *RBOHD*, *FRK1* or *WRKY29* in *eds1-2* BIR1 L1b **(d)** and *pad4-1* BIR1 L0 **(e)**

1018 plants. Photographs and samples for qRT-PCR were taken after 12 days of 30 µM DEX
1019 treatment. Measures were done in mock-treated (DEX-) versus DEX-treated (DEX+) using the
1020 same set of replicates from each genotype. Values from biologically independent samples were
1021 normalized to the *CBP20* internal control, and related to mock-treated plants, set to a value of
1022 1. Data are mean ± SD analyzed by Mann-Whitney test; *, p <0.05. Experiments were repeated
1023 at least twice with similar results.

1024

1025 **Figure 7**

1026 Phenotypes caused by *BIR1* overexpression are independent of salicylic acid (SA)-mediated
1027 signaling pathways. **(a)** Western blot analysis of BIR1-mCherry proteins in the dexamethasone
1028 (DEX)-inducible BIR1-mCherry transgenic Arabidopsis lines wild-type (WT) BIR1 L9, *sid2-*
1029 *2* BIR1 L5 and *eds5-3* BIR1 L10 plants treated with DEX for 7 days. Each sample is a pool of
1030 two plants, and three samples per genotype are shown. Protein loading control by Ponceau S is
1031 shown. **(b)** Morphology of representative *sid2-2* BIR1 L5 and *eds5-3* BIR1 L10 plants. Images
1032 from independent transgenic lines are shown in Figure S8. **(c)** RT-qPCR analysis of *BIR1*
1033 transcripts in *sid2-2* BIR1 L5 and *eds5-3* BIR1 L10 mutant lines. **(d)** RT-qPCR analysis of PR1
1034 transcripts in *eds1-2* BIR1 L1b, *pad4-1* BIR1 L0, *sobir1-12* BIR1 L6, *bak1*-5 BIR1 L10, *sid2-*
1035 *2* BIR1 L5 and *eds5-3* BIR1 L10 mutant lines. Photographs and samples for qRT-PCR were
1036 taken after 12 days of 30 µM DEX treatment Measures were done in mock-treated (DEX-)
1037 versus DEX-treated (DEX+) using the same set of replicates from each genotype. Values from
1038 biologically independent samples were normalized to the *CBP20* internal control, and related
1039 to mock-treated plants, set to a value of 1. Data are mean ± SD analyzed by Mann-Whitney test;
1040 *, p <0.05. Experiments were repeated at least twice with similar results.

1041

1042 **Figure 8**

1043 Expression analyses of phytohormone-related genes in *BIR1* overexpressing plants. **(a, b, c)**
1044 RT-qPCR analysis of *PDF1.2* (a), *PR4* (b), *PAD3* and *CYP79B2* (c) transcripts in *sobir1-12*
1045 BIR1 L6, *bak1*-5 BIR1 L10, *eds1-2* BIR1 L1b, *pad4-1* BIR1 L0, *sid2-2* BIR1 L5 and *eds5-3*
1046 BIR1 L10 mutant lines. Measures were done in mock-treated (DEX-) versus DEX-treated
1047 (DEX+) using the same set of replicates from each genotype. Values from biologically
1048 independent samples were normalized to the *CBP20* internal control, and related to mock-
1049 treated plants, set to a value of 1. Data are mean ± SD analyzed by Mann-Whitney test; *, p

1050 <0.05. **(d)** Tentative working model for BIR1 homeostasis. SA-mediated transcription of *BIR1*
1051 is regulated by RNA-directed DNA methylation (RdDM) and post-transcriptional RNA
1052 silencing (PTGS) (Guzman-Benito *et al.*, 2019). Loss of *BIR1* regulation leads to constitutive
1053 *BIR1* overexpression. *BIR1* overexpression is sensed by one or several TIR1-containing
1054 nucleotide-binding domain leucine-rich repeat receptors (TNLs), of which *CSA1* is a plausible
1055 candidate, to promote *PAD4*-dependent up-regulation of immune-related and defense hormone
1056 genes. TNL activation also leads to effector triggered immunity (ETI)-type cell death that
1057 requires *EDS1* and *SOBIR1*.

1058

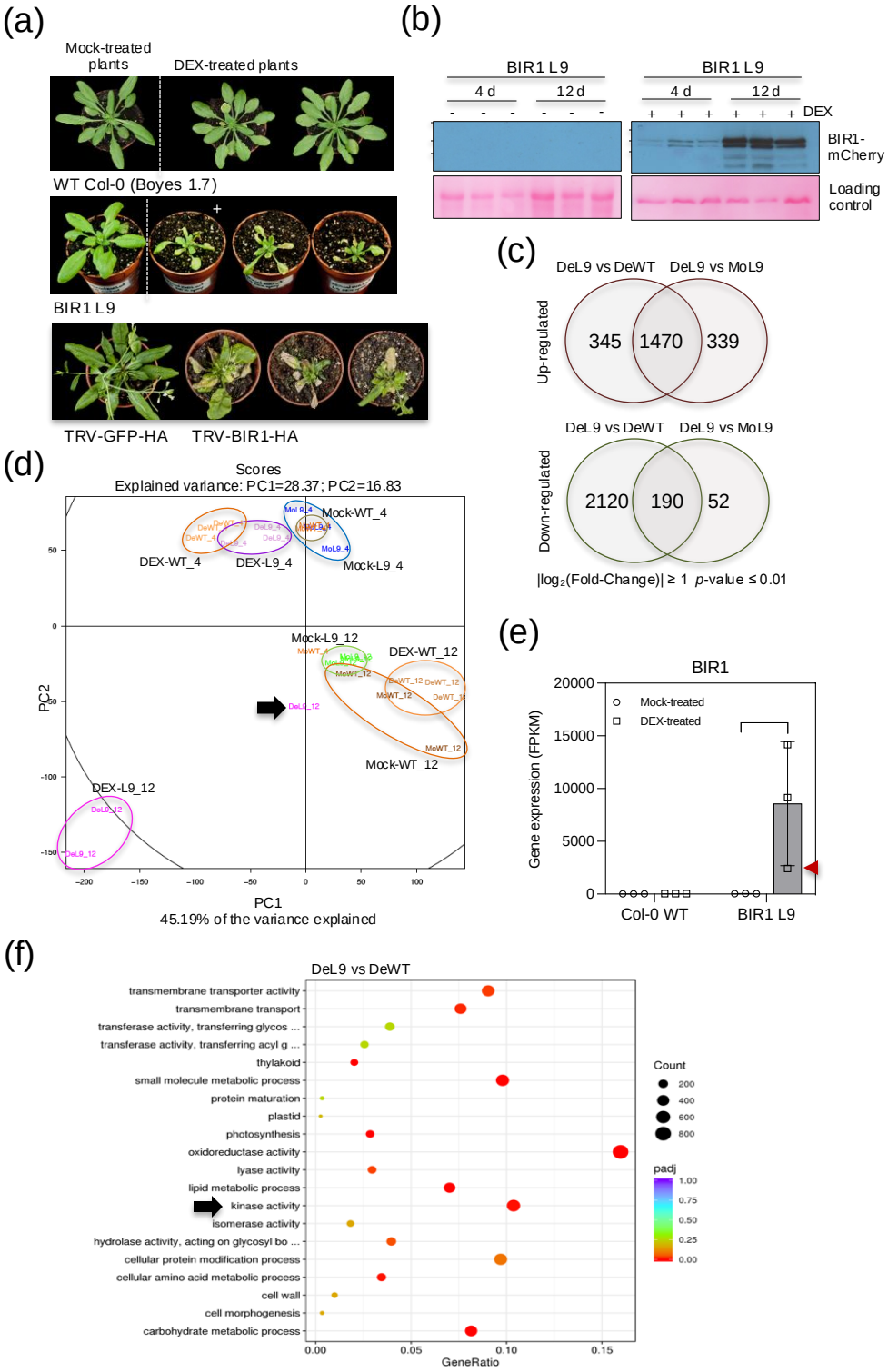

Figure 1

Transcriptional reprogramming associated with *BIR1* induction in Arabidopsis. **(a)** Morphology of representative dexamethasone (DEX)-inducible BIR1-mCherry transgenic Arabidopsis plants from line 9 (L9). Photographs were taken after 10-12 days of 30 µM DEX. Mock-treated wild-type (WT) Arabidopsis were used as controls. DEX treatments started at the Boyes growth stage 1.7. Cell-death phenotypes in Arabidopsis DEX-treated BIR1 L9 plants were similar to those observed when BIR1-HA was expressed via TRV infection (TRV-BIR1). **(b)** Western blot using anti-mCherry antibody shows the relative accumulation of BIR1-mCherry protein after 4 and 12 days of DEX treatments in BIR1 L9 plants. **(c)** Number of up-or down-regulated transcripts, with a $|\log_2(\text{Fold-Change})| \geq 1$ and adjusted *p*-value ≤0.01, in each pairwise comparison is indicated. **(d)** Principal component analysis (PCA) of RNA-Seq data. The PCA was performed using normalized RNA-Seq data of differentially expressed genes (DEGs) under each condition: Mock-treated WT (Mock-WT), Mock-treated BIR1 L9 (Mock-L9), DEX-treated WT (DEX-WT), DEX-treated BIR1 L9 (DEX-L9). Samples were collected after 4 and 12 days of DEX treatment as indicated. Each biological replicate is represented in the score plot. The variance explained by each component (%) is given in parentheses. The sample (DeL9_12b) with differential expression within the DEX-treated L9 group is indicated with an arrow. **(e)** Relative expression of the BIR1-coding gene based on the number of Fragments Per Kilobase of transcript sequence per Millions of base-pairs sequenced (FPKM) (top). Significant differences between DEX- and mock-treated samples were analyzed using two-way ANOVA followed by Sidak´s multiple comparison test; ***, adjusted *p*-value < 0.001. **(f)** Scatterplot of selected gene ontology (GO) terms of DEGs. GO terms between WT and BIR1 L9 plants after 12 days of DEX-treatment (DeL9_ vs DeWT_) are shown. Dot size represents the count of different genes and the color indicates significance of the term enrichment. GO terms with adjusted *p*-value < 0.05 are significantly enriched. The kinase term (indicated by an arrow) was exclusively assigned to BIR1 L9 plants.

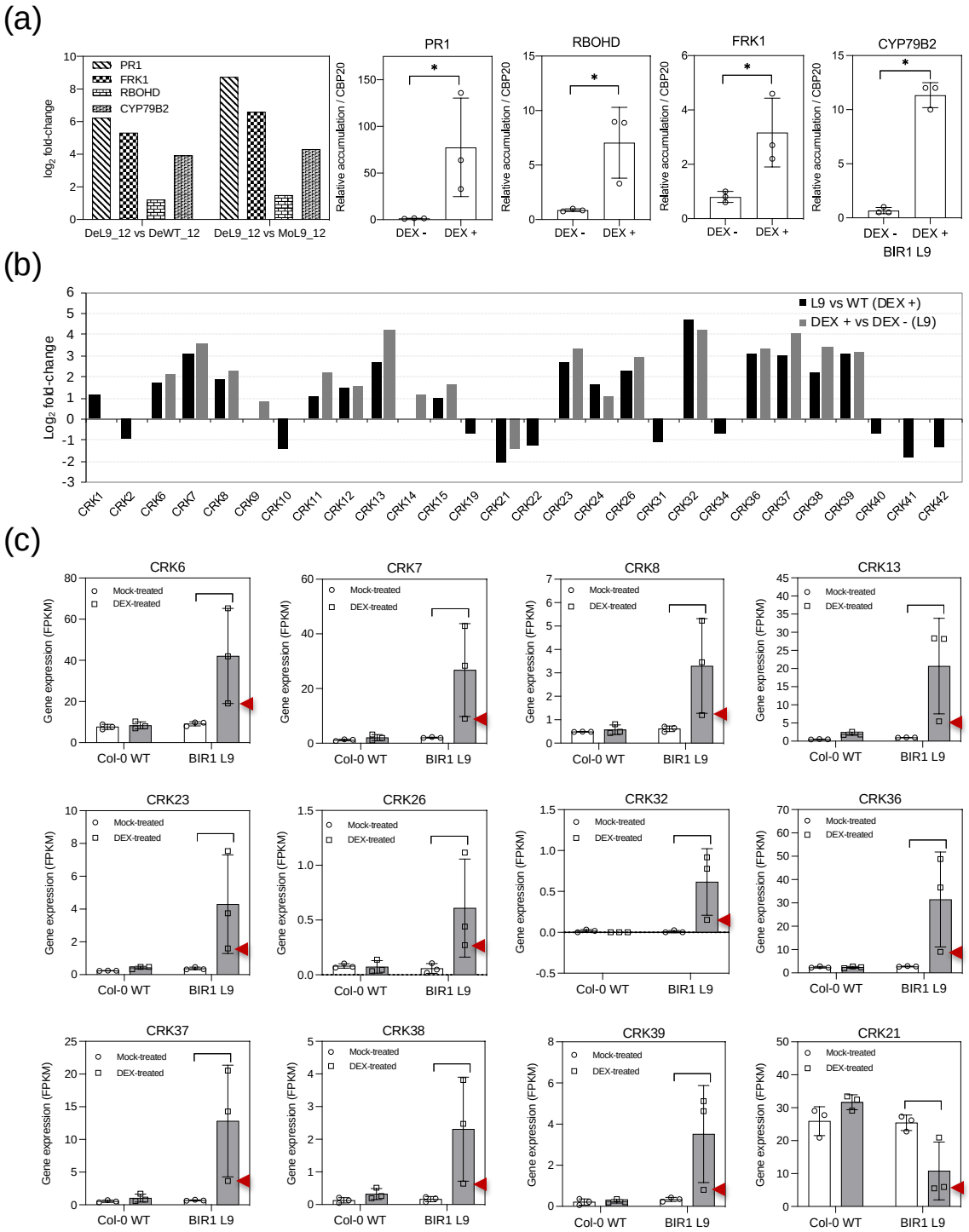

Figure 2

Differential expression of cysteine-rich receptor-like kinase (CRK)-coding genes in *BIR1* overexpressing plants. **(a)** Expression of selected BIR1-responsive differentially expressed genes (DEGs) based on fold-change values (log_2 DeL9_12/DeWT_12 and log_2 DeL9_12/MoL9_12 as indicated) was confirmed by RT-qPCR. Values from biologically independent samples were normalized to the *CBP20* internal control, and related to untreated (DEX-) plants, set to a value of 1. Data are mean ± SD analyzed by Mann-Whitney test; *, p <0.05. **(b)** Expression of CRK-coding differentially expressed genes based on log_2 fold-change in BIR1 overexpressing plants as indicated. (**c)** Relative expression levels of CRK-coding genes represented by the number of Fragments Per Kilobase of transcript sequence per Millions of base-pairs sequenced (FPKM) in each of the three independent samples per condition used for RNA-Seq. Significant differences between dexamethasone (DEX)- and mock-treated samples were analyzed using two-way ANOVA followed by Sidak´s multiple comparison test; ***, adjusted p-value < 0.001, **< 0.01. Note that the expression levels of each individual replicate within the DEX-treated BIR1 L9_12 group mirror the abundance of *BIR1* transcripts in each replicate. Values from the DeL9_12b sample are indicated by an arrowhead.

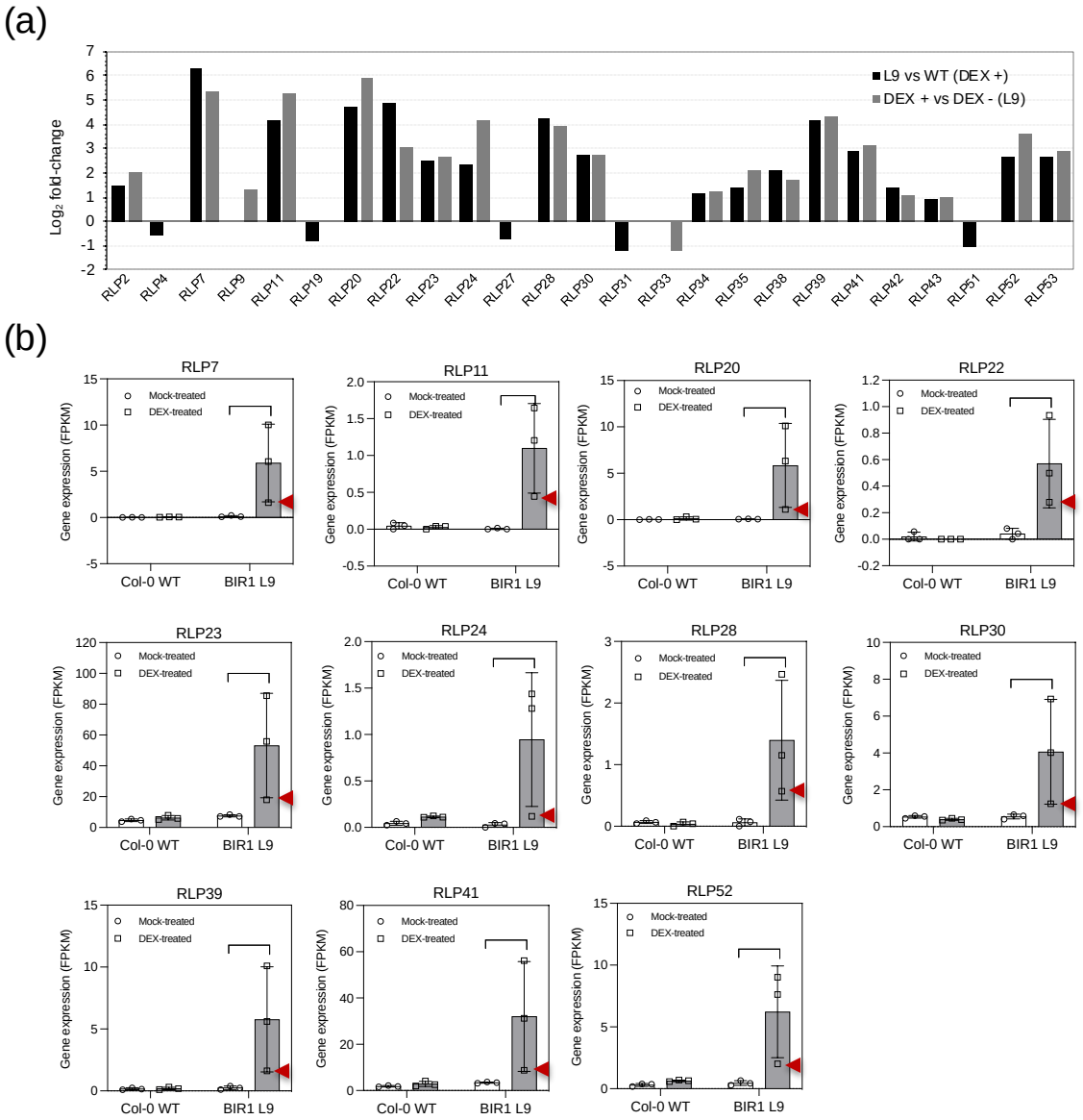

Figure 3

Differential expression of receptor-like protein (RLP)-coding genes in *BIR1* overexpressing plants. **(a)** Expression of differentially expressed RLP-coding genes based on $\log_2$ fold-change as indicated. **(b)** Relative expression levels of RLP-coding genes represented by the number of Fragments Per Kilobase of transcript sequence per Millions of base-pairs sequenced (FPKM) in each of the three independent samples per condition used for RNA-Seq. Significant differences between dexamethasone (DEX)- and mock-treated samples were analyzed using two-way ANOVA followed by Sidak's multiple comparison test; ***, adjusted *p*-value < 0.001, **< 0.01. Note that the expression levels of each individual replicate within the DEX-treated BIR1 L9_12 group mirror the abundance of *BIR1* transcripts in each replicate. Values from the DeL9_12b sample are indicated by an arrowhead.

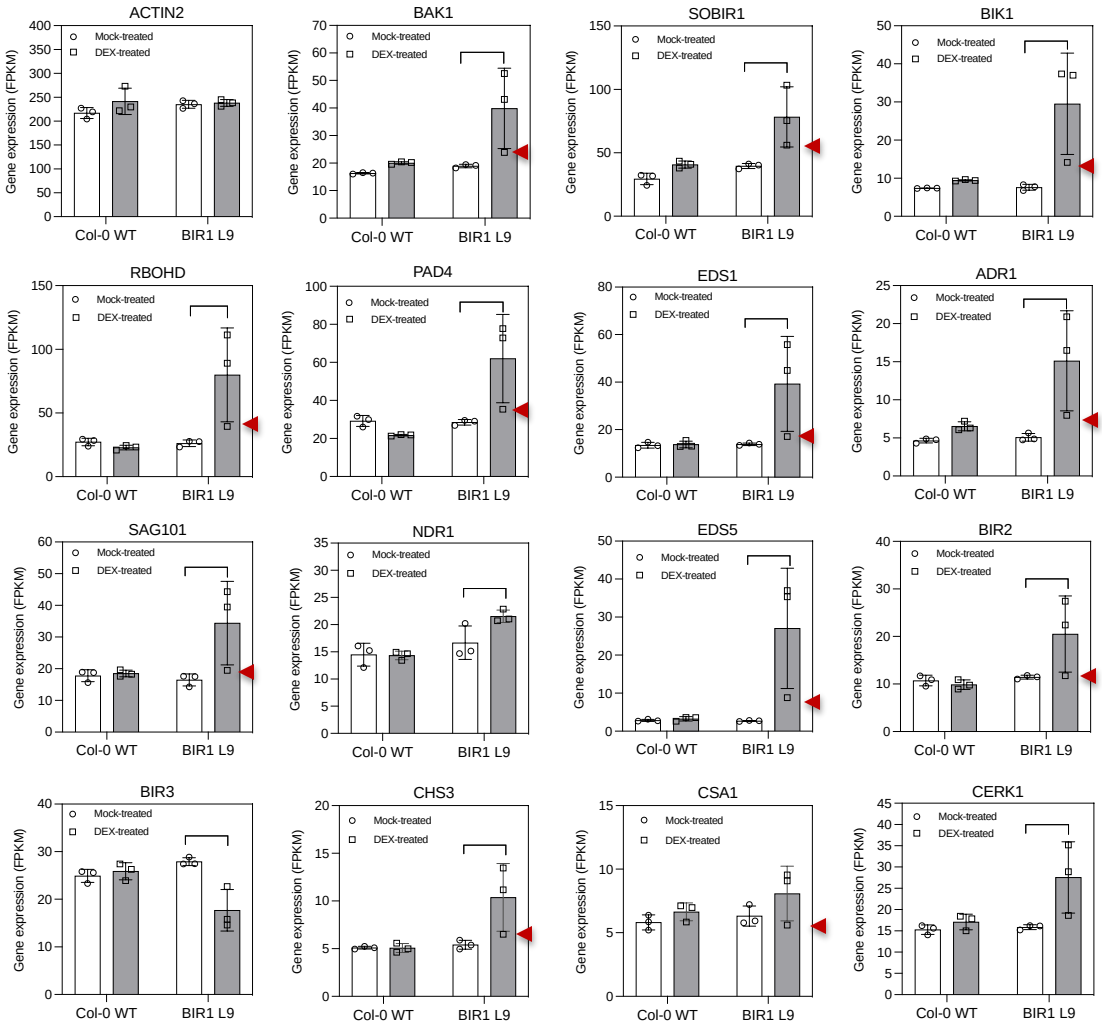

Figure 4

BIR1 overexpression leads to the transcriptional activation of pattern-triggered immunity (PTI)-associated co-receptors and effector-triggered immunity (ETI) regulators. Relative expression of selected genes encoding PTI/ETI-markers based on the number of Fragments Per Kilobase of transcript sequence per Millions of base-pairs sequenced (FPKM) in each of the three independent samples per condition used for RNA-Seq. Actin expression is shown as control. Note that the expression levels of each individual replicate within the DEX-treated BIR1 L9_12 group mirror the abundance of *BIR1* transcripts in each replicate. DeL9_12b is indicated by a red arrow. Significant differences between mock-treated and DEX-treated samples were analyzed using two-way ANOVA followed by Sidak´s multiple comparison test; **, adjusted *p*-value < 0.01, * < 0.05. Values from the DeL9_12b sample are indicated by an arrowhead.

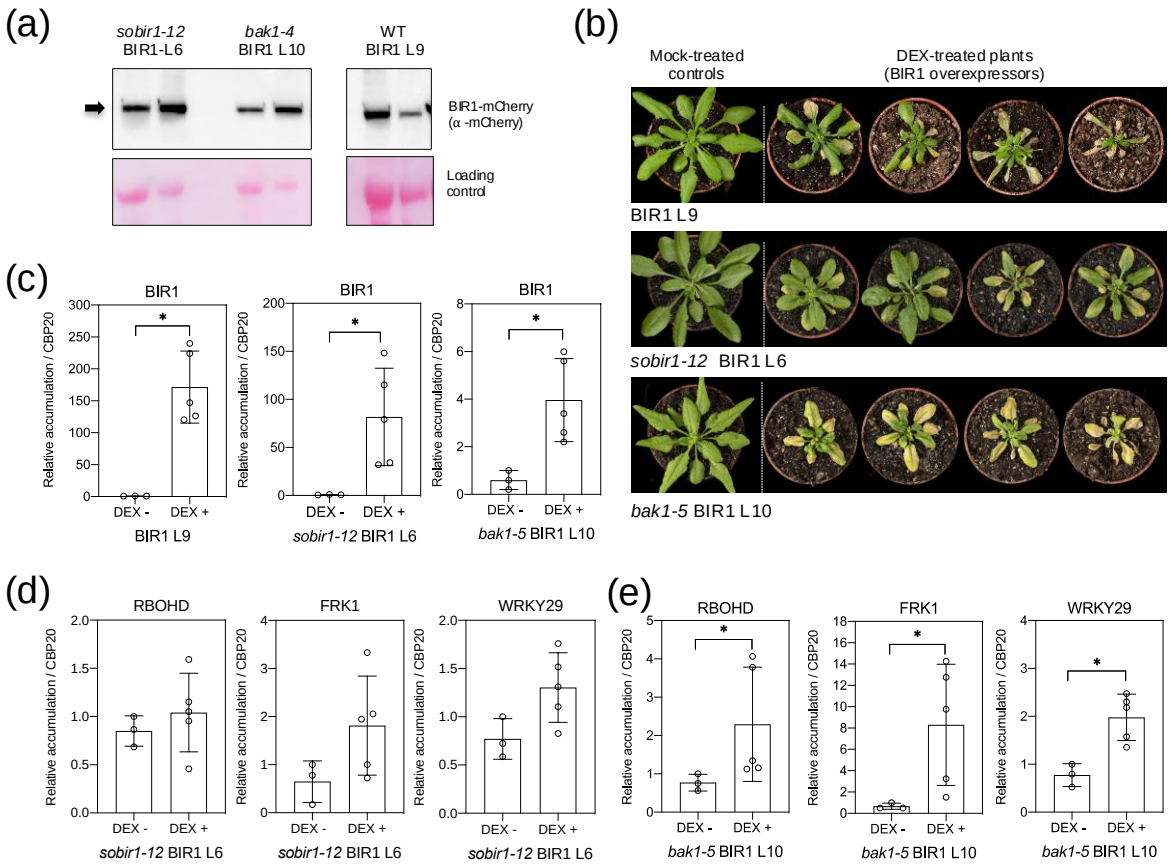

Figure 5

Phenotypes caused by *BIR1* overexpression are partially rescued in *sobir1-12* mutants. **(a)** Western blot analysis of BIR1-mCherry proteins in the dexamethasone (DEX)-inducible BIR1-mCherry transgenic Arabidopsis lines wild-type (WT) BIR1 L9, *sobir1-12* BIR1 (L6) and *bak1*-5 BIR1 (L10) plants treated with DEX for 7 days. Each sample is a pool of two plants, and three samples per genotype are shown. Protein loading control by Ponceau S is shown. A composite image is shown. **(b)** Morphology of representative WT BIR1 L9, *sobir1-12* BIR1 L6 and *bak1*-5 BIR1 L10 plants. Images from independent transgenic lines are shown in **Figure S8**. **(c)** RT-qPCR analysis of *BIR1* transcripts in WT BIR1 L9, *sobir1-12* BIR1 L6 and *bak1*-5 BIR1 L10 plants. **(d, e)** RT-qPCR analysis of PTI-markers *RBOHD*, *FRK1* or *WRKY29* in *sobir1-12* BIR1 L6 **(d)** and *bak1*-5 BIR1 L10 **(e)** plants. Photographs and samples for qRT-PCR were taken after 12 days of 30 µM DEX treatment. Measures were done in mock-treated (DEX-) versus DEX-treated (DEX+) using the same set of replicates from each genotype. Values from biologically independent samples were normalized to the *CBP20* internal control, and related to mock-treated plants, set to a value of 1. Data are mean ± SD analyzed by Mann-Whitney test; *, p <0.05. Experiments were repeated at least twice with similar results.

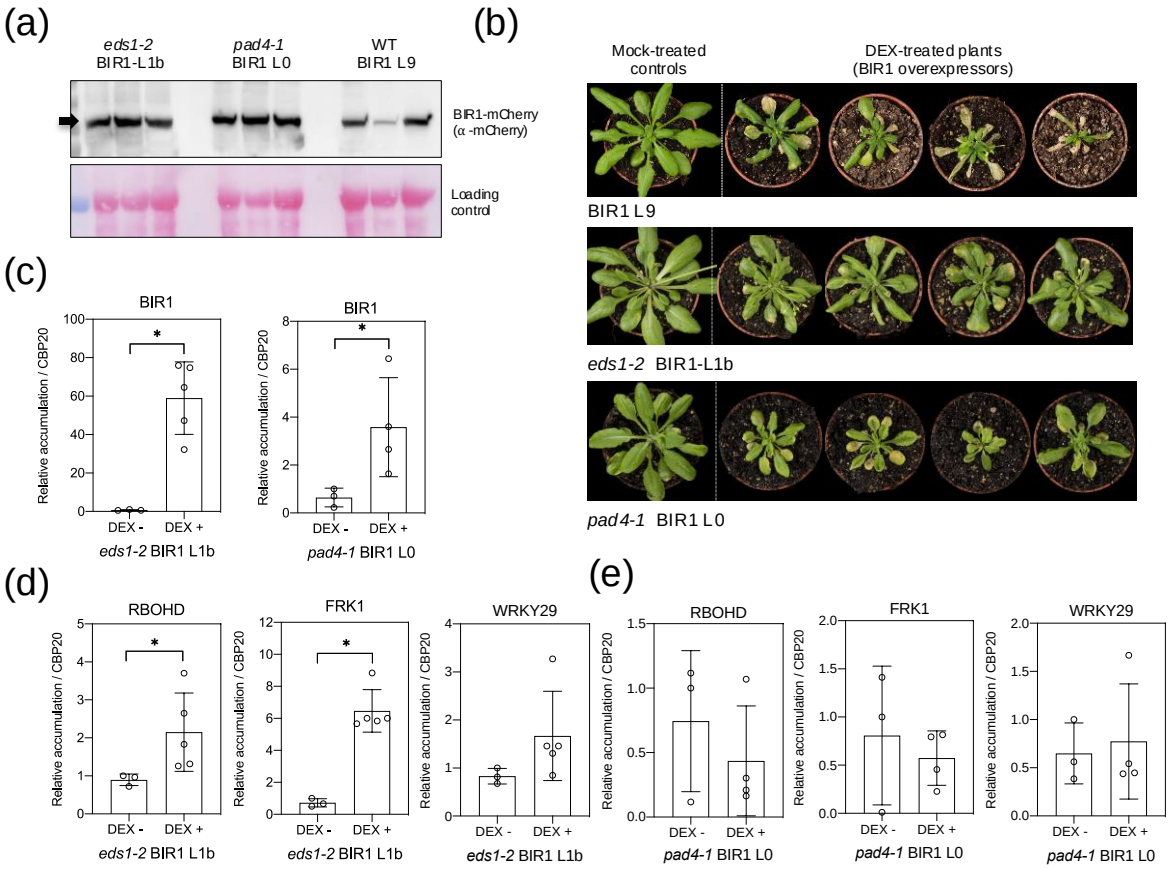

Figure 6

Phenotypes caused by *BIR1* overexpression are partially rescued in *eds1-2* mutants, but not in *pad4-1* mutants. **(a)** Western blot analysis of BIR1-mCherry proteins in the dexamethasone (DEX)-inducible BIR1-mCherry transgenic Arabidopsis lines wild-type (WT) BIR1 L9, *eds1-2* BIR1 L1b and *pad4-1* BIR1 L0 plants treated with DEX for 7 days. Each sample is a pool of two plants, and three samples per genotype are shown. Protein loading control by Ponceau S is shown. **(b)** Morphology of representative *eds1-2* BIR1 L1b and *pad4-1* BIR1 L0 plants. Images from independent transgenic lines are shown in Figure S8. **(c)** RT-qPCR analysis of *BIR1* transcripts in *eds1-2* BIR1 L1b and *pad4-1* BIR1 L0 mutant lines. **(d, e)** RT-qPCR analysis of PTI-markers *RBOHD*, *FRK1* or *WRKY29* in *eds1-2* BIR1 L1b **(d)** and *pad4-1* BIR1 L0 **(e)** plants. Photographs and samples for qRT-PCR were taken after 12 days of 30 µM DEX treatment. Measures were done in mock-treated (DEX-) versus DEX-treated (DEX+) using the same set of replicates from each genotype. Values from biologically independent samples were normalized to the *CBP20* internal control, and related to mock-treated plants, set to a value of 1. Data are mean ± SD analyzed by Mann-Whitney test; *, $p < 0.05$. Experiments were repeated at least twice with similar results.

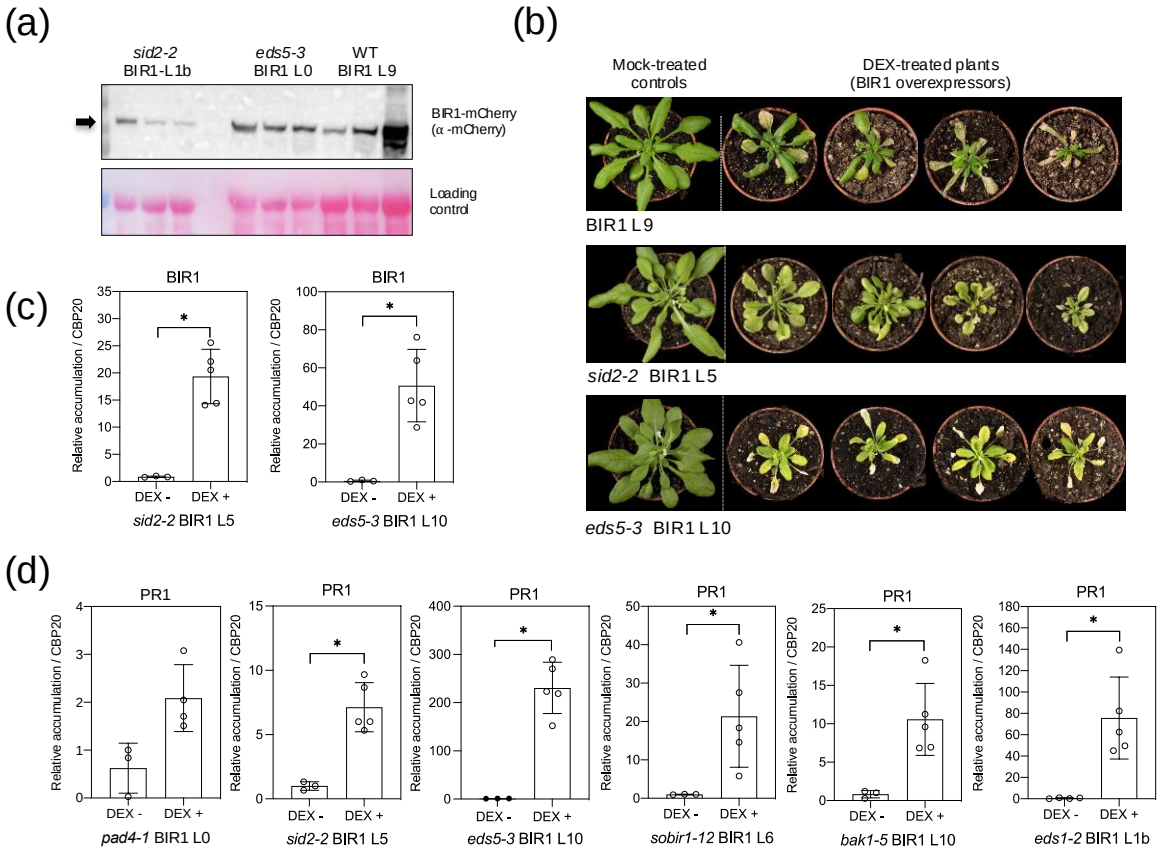

Figure 7

Phenotypes caused by *BIR1* overexpression are independent of salicylic acid (SA)-mediated signaling pathways. **(a)** Western blot analysis of BIR1-mCherry proteins in the dexamethasone (DEX)-inducible BIR1-mCherry transgenic Arabidopsis lines: wild-type (WT) BIR1 L9, *sid2-2* BIR1 L5 and *eds5-3* BIR1 L10 plants treated with DEX for 7 days. Each sample is a pool of two plants, and three samples per genotype are shown. Protein loading control by Ponceau S is shown. **(b)** Morphology of representative *sid2-2* BIR1 L5 and *eds5-3* BIR1 L10 plants. Images from independent transgenic lines are shown in Figure S8. **(c)** RT-qPCR analysis of *BIR1* transcripts in *sid2-2* BIR1 L5 and *eds5-3* BIR1 L10 mutant lines. **(d)** RT-qPCR analysis of PR1 transcripts in *eds1-2* BIR1 L1b, *pad4-1* BIR1 L0, *sobir1-12* BIR1 L6, *bak1*-5 BIR1 L10, *sid2-2* BIR1 L5 and *eds5-3* BIR1 L10 mutant lines. Photographs and samples for qRT-PCR were taken after 12 days of 30 µM DEX treatment Measures were done in mock-treated (DEX-) versus DEX-treated (DEX+) using the same set of replicates from each genotype. Values from biologically independent samples were normalized to the CBP20 internal control, and related to mock-treated plants, set to a value of 1. Data are mean ± SD analyzed by Mann-Whitney test; *, p <0.05. Experiments were repeated at least twice with similar results.

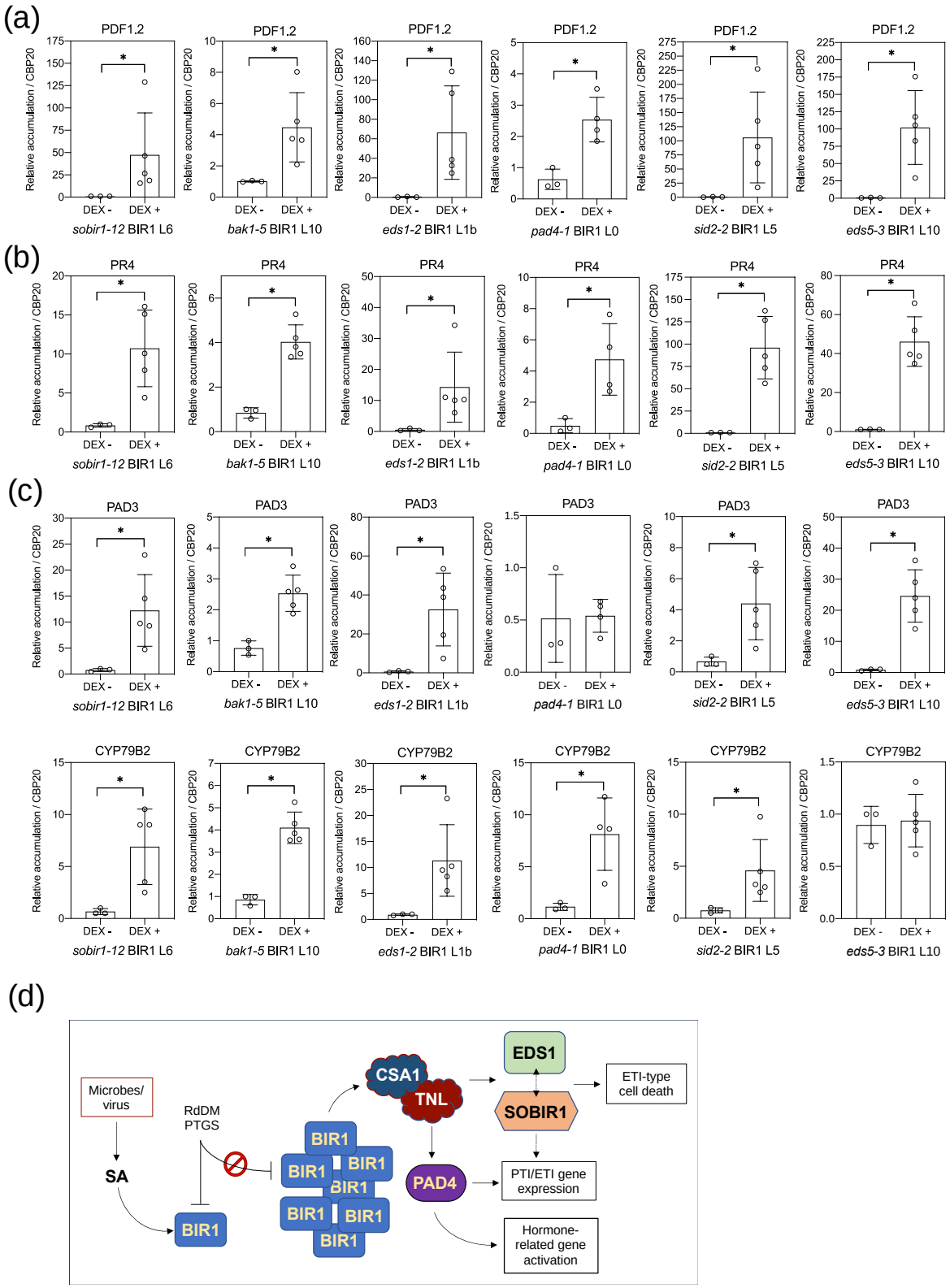

Figure 8

Expression analyses of phytohormone-related genes in *BIR1* overexpressing plants. **(a, b, c)** RT-qPCR analysis of *PDF1.2* (a), *PR4* (b), *PAD3* and *CYP79B2* (c) transcripts in *sobir1-12* BIR1 L6, *bak1*-5 BIR1 L10, *eds1-2* BIR1 L1b, *pad4-1* BIR1 L0, *sid2-2* BIR1 L5 and *eds5-3* BIR1 L10 mutant lines. Measures were done in mock-treated (DEX-) versus DEX-treated (DEX+) using the same set of replicates from each genotype. Values from biologically independent samples were normalized to the CBP20 internal control, and related to mock-treated plants, set to a value of 1. Data are mean ± SD analyzed by Mann-Whitney test; *, p <0.05. **(d)** Tentative working model for BIR1 homeostasis. SA-mediated transcription of *BIR1* is regulated by RNA-directed DNA methylation (RdDM) and post-transcriptional RNA silencing (PTGS) (Guzman-Benito *et al.*, 2019). Loss of *BIR1* regulation leads to constitutive *BIR1* overexpression. *BIR1* overexpression is sensed by one or several TIR1-containing nucleotide-binding domain leucine-rich repeat receptors (TNLs), of which *CSA1* is a plausible candidate, to promote *PAD4*-dependent up-regulation of immune-related and defense hormone genes. TNL activation also leads to effector triggered immunity (ETI)-type cell death that requires *EDS1* and *SOBIR1*.

SUPPORTING INFORMATION

Article title:

Overexpression of the receptor-like kinase *BIR1* gene causes *SOBIR1*- and *EDS1*-dependent cell death phenotypes in Arabidopsis

Irene Guzmán-Benito[1,2], Carmen Robinson[1,3], Isabel Punzón[1], César Llave[1,*]

1. Centro de Investigaciones Biológicas Margarita Salas. Consejo Superior de Investigaciones Científicas, Ramiro de Maeztu 9, 28040 Madrid, Spain
2. Current address. Department of Plant Molecular Biology, University of Lausanne, 1015 Lausanne, Switzerland
3. Doctorado en Biotecnología y Recursos Genéticos de Plantas y Microorganismos Asociados, Universidad Politécnica de Madrid, 28040 Madrid, Spain

The following Supporting data is available for this article:

Figure S1. Transcriptomic profiling of dexamethasone (DEX)-treated wild-type Col-0 plants.

Figure S2. Transcriptomic profiling of BIR1 expressing transgenic lines.

Figure S3. Enrichment analysis of Kyoto Encyclopedia of Genes and Genomes (KEGG) pathways using RNA-Seq data.

Figure S4. Differential expression of cell-surface pattern recognition receptors (PRR)-coding genes in BIR1 overexpressing plants.

Figure S5. Differential expression of calcium-dependent protein kinases (CPK)-coding genes in BIR1 overexpressing plants.

Figure S6. Differential expression of HETEROTRIMERIC G PROTEIN-coding genes in BIR1 overexpressing plants.

Figure S7. Morphological and growth defects in dexamethasone (DEX)-treated *BIR1* overexpressing plants of different immune mutant genetic backgrounds.

Figure S8. Morphological phenotypes of dexamethasone (DEX)-treated PTI/ETI mutant genetic backgrounds and mCherry transgenic plants.

Table S1. List of primers

Table S2. List of expressed genes.

Table S3. List of differentially expressed genes (DEG. padjust value < 0.05).

Table S4. List of differentially expressed genes (DEG. |Log_2fold change > 1| padjust value < 0.01).

Table S5. Enrichment analysis of Gene Ontology (GO) terms.

Table S6. Kyoto Encyclopedia of Genes and Genomes (KEGG) pathway enrichment analysis.

Table S7. List of differentially expressed genes (DEG. padjust value < 0.05) within functional categories.

Table S8. Statistical analysis of enrichment of functional gene groups in plants overexpressing BIR1 after 12 days of DEX treatment relative to non-expressing controls using Two-tailed Fisher's exact tests.

SUPPORTING FIGURES

Figure S1

Transcriptomic profiling of dexamethasone (DEX)-treated wild-type (WT) Col-0 plants. **(a)** Morphology of representative WT Arabidopsis plants after 10-12 days of 30 µM DEX treatment. Mock-treated plants are shown as controls. DEX treatments started at the Boyes growth stages 1.5 or 1.7, as indicated. Rosette size (diameter) in WT (Boyes 1.5 and 1.7) after 12 days of DEX treatment relative to mock-treated controls is shown. Box and whisker plots showing 5-95 percentile were analyzed by Mann-Whitney test; ****, p <0.0001. **(b)** Volcano plots showing the distribution of differentially expressed genes (DEGs) (adjusted *p*-value ≤ 0.05). The x-axis shows the gene fold change, and y-axis plots the statistical significance (*p*-value) of the differences. Significantly up- and down-regulated genes are highlighted in red and green, respectively. Genes that are not differentially regulated are in blue. **(c)** Scatterplot of selected gene ontology (GO) terms of DEGs. GO terms between DEX-treated and mock-treated WT plants at 12 days of treatment (DeL9_ vs MoL9_) are shown. Dot size represents the count

of different genes and the color indicates significance of the term enrichment. GO terms with adjusted *p*-value < 0.05 are significantly enriched. WT, wild-type Col-0; De, DEX-treated plants; Mo, Mock-treated plants; _12, 12 days of treatment.

Figure S2

Transcriptomic profiling of *BIR1* expressing transgenic lines. **(a)** Number of up-or down-regulated transcripts, with a $|\log_2 (\text{Fold-Change})| \geq 1$ and adjusted *p*-value ≤0.05, in each pairwise comparison as indicated. **(b)** Volcano plots showing the distribution of DEGs (adjusted *p*-value ≤ 0.05). The x-axis shows the fold change in gene expression between samples, and y-axis shows the statistical significance of the differences. Significantly up- and down-regulated genes are highlighted in red and green, respectively. Genes that are not differentially regulated are in blue. **(c)** Scatterplot of selected gene ontology (GO) terms of DEGs. GO terms between wild-type (WT) and BIR1 L9 plants at 12 days after DEX-treatment (DeL9_ vs MoL9_) are shown. Dot size represents the count of different genes and the color indicates significance of the term enrichment. GO terms with adjusted *p*-value < 0.05 are significantly enriched. The kinase term (indicated by an arrow) was exclusively assigned to BIR1 L9 plants. WT, wild-type Col-0; L9, BIR1 L9 transgenic plants; De, DEX-treated plants; Mo, Mock-treated plants; _12, 12 days of treatment.

Figure S3

Enrichment analysis of Kyoto Encyclopedia of Genes and Genomes (KEGG) pathways using RNA-Seq data. Scatterplot of selected Kyoto Encyclopedia of Genes and Genomes (KEGG) pathways. Dot size represents the count of different genes and the color indicates significance of the term enrichment. Terms with adjusted *p*-value < 0.05 are significantly enriched. WT, wild-type Col-0; De, DEX-treated plants; Mo, Mock-treated plants; _12, 12 days of treatment.

Figure S4

Differential expression of cell-surface pattern recognition receptors (PRR)-coding genes in *BIR1* overexpressing plants. **(a)** Relative expression levels are represented by the number of Fragments Per Kilobase of transcript sequence per Millions of base-pairs sequenced (FPKM) in each of the three independent samples per condition used for RNA-Seq. Significant

differences between dexamethasone (DEX)- and mock-treated samples were analyzed using two-way ANOVA followed by Sidak´s multiple comparison test; *, adjusted *p*-value < 0.05. **(b)** Western blot analysis of EDS1, SOBIR1 and PR1 using specific antibodies in two independent sets of BIR1 L9 samples. Plants were mock-treated (-) or DEX-treated (+) for 12 days. Protein loading control by Ponceau S is shown.

Figure S5

Differential expression of calcium-dependent protein kinases (CPK)-coding genes in *BIR1* overexpressing plants. Relative expression levels are represented by the number of Fragments Per Kilobase of transcript sequence per Millions of base-pairs sequenced (FPKM) in each of the three independent samples per condition used for RNA-Seq. Significant differences between dexamethasone (DEX)- and mock-treated samples were analyzed using two-way ANOVA followed by Sidak´s multiple comparison test; **, adjusted *p*-value < 0.01, *< 0.05.

Figure S6

Differential expression of *HETEROTRIMERIC G PROTEIN* genes in *BIR1* overexpressing plants. Relative expression levels are represented by the number of Fragments Per Kilobase of transcript sequence per Millions of base-pairs sequenced (FPKM) in each of the three independent samples per condition used for RNA-Seq. Significant differences between dexamethasone (DEX)- and mock-treated samples were analyzed using two-way ANOVA followed by Sidak´s multiple comparison test; *, adjusted *p*-value < 0.05.

Figure S7

Morphological and growth defects in independent dexamethasone (DEX)-treated *BIR1* overexpressing plants of different immune mutant genetic backgrounds. **(a)** Morphology of representative DEX-inducible BIR1-mCherry transgenic Arabidopsis lines in *sobir1-12* (*sobir1-12* BIR1 L8), *bak1*-5 (*bak1*-5 BIR1 L4), *eds1*-2 (*eds1*-2 BIR1 L2), *pad4-1* (*pad4-1* BIR1 L12b) and *eds5-3* (*eds5-3* BIR1 L12) backgrounds. Photographs were taken after 10-12 days of 30 µM DEX treatment. Mock-treated plants are shown as controls. **(b)** Morphology and *BIR1* expression levels of DEX-treated and mock-treated *sobir1-12* BIR1 (L6, L8) and *bak1-5* BIR1 (L4, L10) plants as observed in a different repetition of the experiment. **(c)** Western blot

123 analysis of BIR1-mCherry in the genotypes indicated. Plants were mock-treated (-) or DEX-
124 treated (+) for 12 days. Protein loading control by Ponceau S is shown (left panel). qRT-PCR
125 analysis showed comparable *BIR1* transcript levels in both genotypes. Each sample consisted
126 of RNA pooled from six different plants (right panel).

127

128 **Figure S8**

129 Morphological phenotypes of dexamethasone (DEX)-treated immune mutant genetic
130 backgrounds and mCherry transgenic plants. Morphology of BIR1 L9, *sobir1-12*, *bak1-5, eds1-*
131 *2*, *pad4-1*, *sid2-2* and *eds5-3* mutant plants and mCherry transgenic Arabidopsis after 12 days
132 of treatment with 30 µM. Mock-treated plants of each genotype are shown as controls.

133

134 **SUPPORTING TABLES**

135 **Table S2**

136 List of expressed genes. Values represent the total read counts/ Fragments Per Kilobase of
137 transcript sequence per Millions of base-pairs sequenced (FRKM) values of each biological
138 replicate (a,b,c) per condition and their corresponding row mean values. De (DEX-treated
139 plants), Mo (Mock-treated plants), WT (wild-type plants), L9 (BIR1 L9 transgenic plants), _4
140 (4 days of treatment), _12 (12 days of treatment)

141

142 **Table S3**

143 List of differentially expressed genes (DEG. padjust value < 0.05). Values represent the mean
144 Fragments Per Kilobase of transcript sequence per Millions of base-pairs sequenced (FPKM)
145 values from three biological replicates per condition. De (DEX-treated plants), Mo (Mock-
146 treated plants), WT (wild-type plants), L9 (BIR1 L9 transgenic plants), _12 (12 days of
147 treatment).

148

149 **Table S4**

150 List of differentially expressed genes (DEG. $|Log_2 fold\ change > 1|$ padjust value < 0.01). Values
151 represent the mean Fragments Per Kilobase of transcript sequence per Millions of base-pairs
152 sequenced (FPKM) values from three biological replicates per condition. De (DEX-treated

153 plants), Mo (Mock-treated plants), WT (wild-type plants), L9 (BIR1 L9 transgenic plants), _12
154 (12 days of treatment).

155

156 **Table S5**

157 Enrichment analysis of Gene Ontology (GO) terms. CC (cellular component), BP (biological
158 process) and MF (molecular function). Gene Ratio is the ratio of DEGs to all genes for this GO
159 term. Bg Ratio is the ratio of all genes concerning this GO term to all genes in background GO
160 database. Count is the number of differentially expressed genes concerning this GO term.
161 Adjusted p-value < 0.05 means significant enrichment. De (DEX-treated plants), Mo (Mock-
162 treated plants), WT (wild-type plants), L9 (BIR1 L9 transgenic plants), _12 (12 days of
163 treatment).

164

165 **Table S6**

166 Kyoto Encyclopedia of Genes and Genomes (KEGG) pathway enrichment analysis. Gene Ratio
167 is the ratio of DEGs to all genes for this pathway. Bg Ratio is the ratio of all genes concerning
168 this KEGG term to all genes in background KEGG database. Count is the number of
169 differentially expressed genes concerning this term. Adjusted p-value < 0.05 means significant
170 enrichment. De (DEX-treated plants), Mo (Mock-treated plants), WT (wild-type plants), L9
171 (BIR1 L9 transgenic plants), _12 (12 days of treatment).

172

173 **Table S7**

174 List of differentially expressed genes (DEG. padjust value < 0.05) within functional categories.
175 Values represent the mean Fragments Per Kilobase of transcript sequence per Millions of base-
176 pairs sequenced (FPKM) values from three biological replicates per condition. De (DEX-
177 treated plants), Mo (Mock-treated plants), WT (wild-type plants), L9 (BIR1 L9 transgenic
178 plants), _12 (12 days of treatment).

179

180 **Table S8**

181 Statistical analysis of enrichment of functional gene groups in plants overexpressing BIR1 after
182 12 days of DEX treatment relative to non-expressing controls using Two-tailed Fisher's exact

183 tests. De (DEX-treated plants), Mo (Mock-treated plants), WT (wild-type plants), L9 (BIR1 L9
184 transgenic plants). LRR, leucine-rich repeat; RLK, receptor-like kinase; CRK, cysteine-rich
185 RLKs; RLP, receptor-like protein; TNL, TIR1-nucleotide-binding domain LRR immune
186 receptors.

187

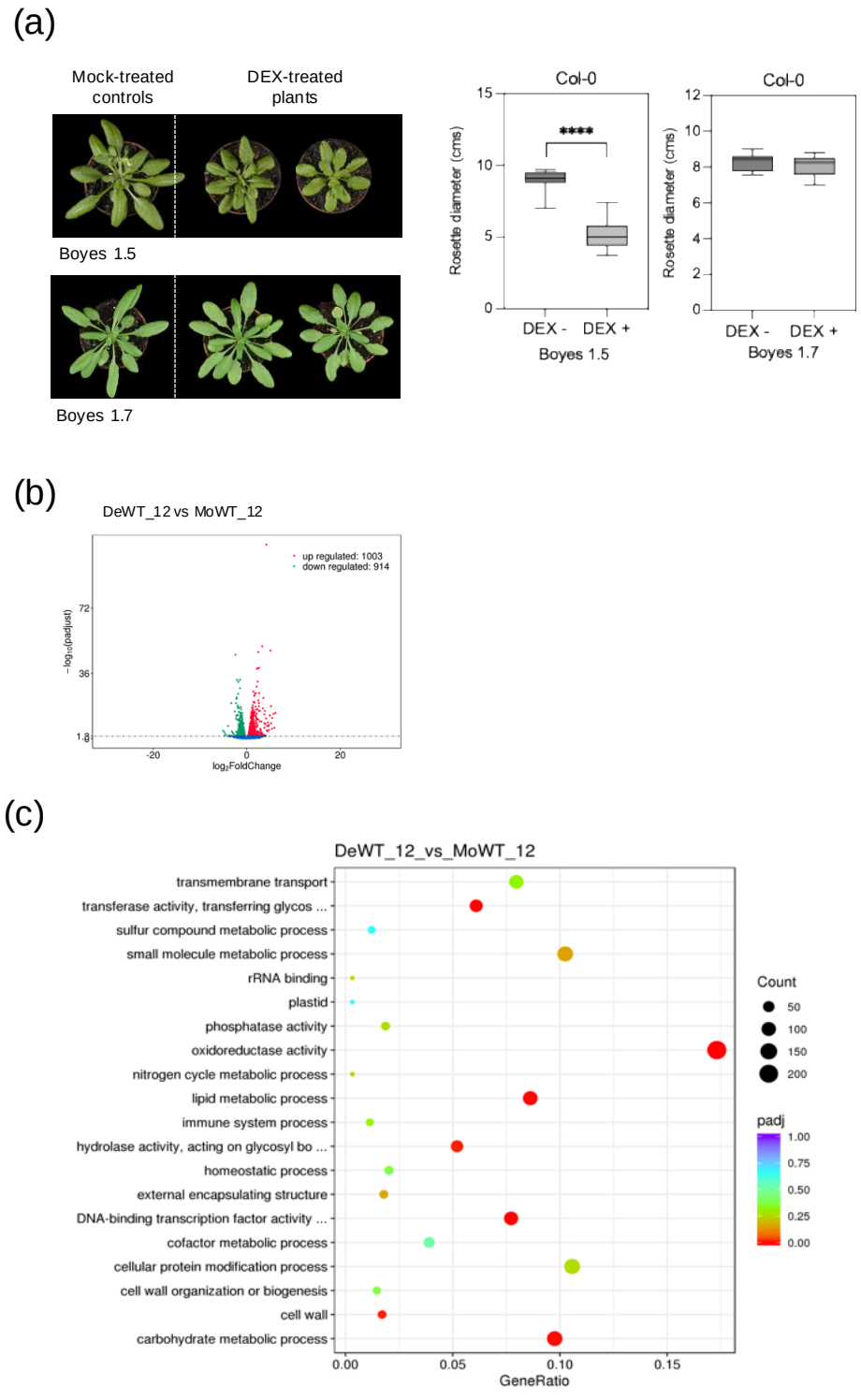

Figure S1

Transcriptomic profiling of dexamethasone (DEX)-treated wild-type (WT) Col-0 plants. **(a)** Morphology of representative WT Arabidopsis plants after 10-12 days of 30 µM DEX treatment. Mock-treated plants are shown as controls. DEX treatments started at the Boyes growth stages 1.5 or 1.7, as indicated. Rosette size (diameter) in WT (Boyes 1.5 and 1.7) after 12 days of DEX treatment relative to mock-treated controls is shown. Box and whisker plots showing 5-95 percentile were analyzed by Mann-Whitney test; ****, p <0.0001. **(b)** Volcano plots showing the distribution of differentially expressed genes (DEGs) (adjusted *p*-value ≤ 0.05). The x-axis shows the gene fold change, and y-axis plots the statistical significance (*p*-value) of the differences. Significantly up- and down-regulated genes are highlighted in red and green, respectively. Genes that are not differentially regulated are in blue. **(c)** Scatterplot of selected gene ontology (GO) terms of DEGs. GO terms between DEX-treated and mock-treated WT plants at 12 days of treatment (DeL9_ vs MoL9_) are shown. Dot size represents the count of different genes and the color indicates significance of the term enrichment. GO terms with adjusted *p*-value < 0.05 are significantly enriched. WT, wild-type Col-0; De, DEX-treated plants; Mo, Mock-treated plants; _12, 12 days of treatment.

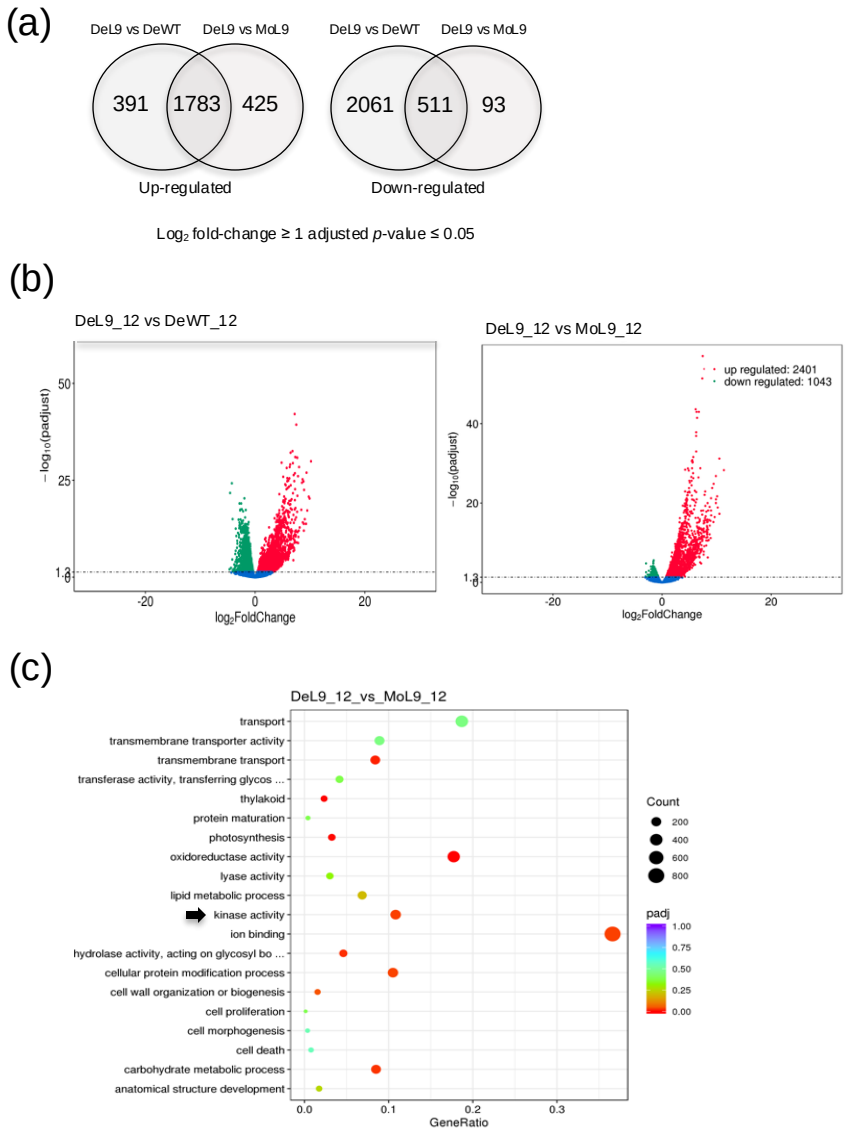

Figure S2

Transcriptomic profiling of *BIR1* expressing transgenic lines. **(a)** Number of up-or down-regulated transcripts, with a $|\log_2(\text{Fold-Change})| \geq 1$ and adjusted *p*-value ≤0.05, in each pairwise comparison as indicated. **(b)** Volcano plots showing the distribution of DEGs (adjusted *p*-value ≤ 0.05). The x-axis shows the fold change in gene expression between samples, and y-axis shows the statistical significance of the differences. Significantly up- and down-regulated genes are highlighted in red and green, respectively. Genes that are not differentially regulated are in blue. **(c)** Scatterplot of selected gene ontology (GO) terms of DEGs. GO terms between wild-type (WT) and BIR1 L9 plants at 12 days after DEX-treatment (DeL9_ vs MoL9_) are shown. Dot size represents the count of different genes and the color indicates significance of the term enrichment. GO terms with adjusted *p*-value < 0.05 are significantly enriched. The kinase term (indicated by an arrow) was exclusively assigned to BIR1 L9 plants. WT, wild-type Col-0; L9, BIR1 L9 transgenic plants; De, DEX-treated plants; Mo, Mock-treated plants; _12, 12 days of treatment.

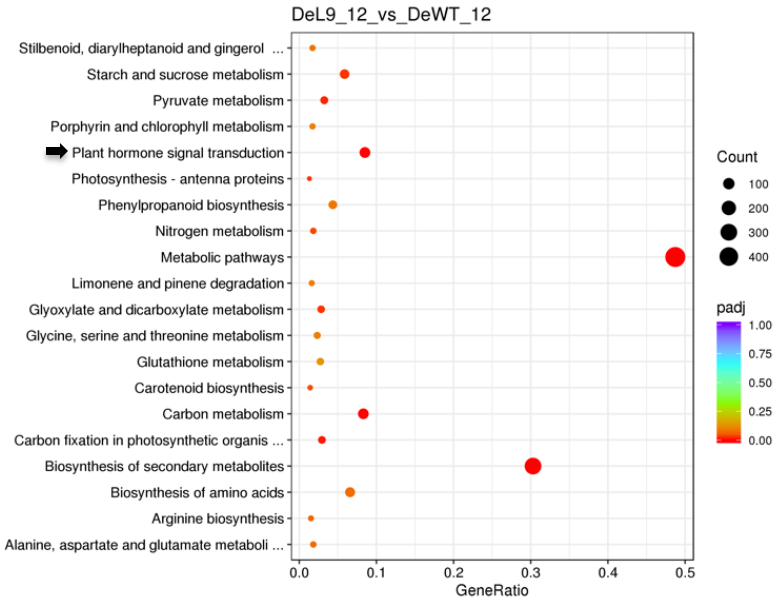

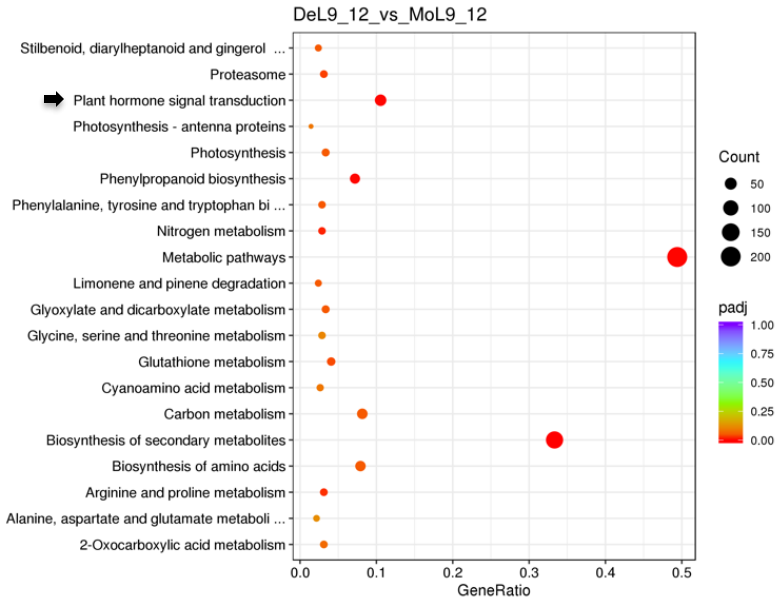

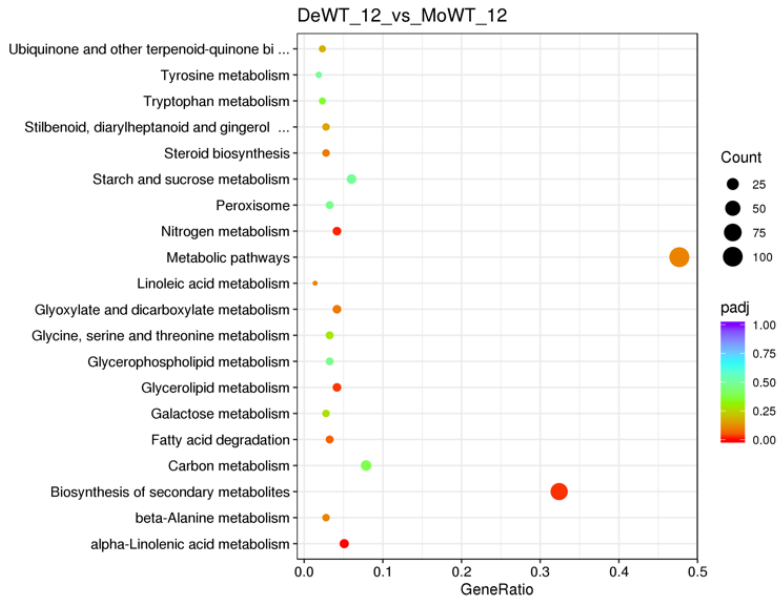

Figure S3

Enrichment analysis of Kyoto Encyclopedia of Genes and Genomes (KEGG) pathways using RNA-Seq data. Scatterplot of selected Kyoto Encyclopedia of Genes and Genomes (KEGG) pathways. Dot size represents the count of different genes and the color indicates significance of the term enrichment. Terms with adjusted *p*-value < 0.05 are significantly enriched. WT, wild-type Col-0; De, DEX-treated plants; Mo, Mock-treated plants; _12, 12 days of treatment.

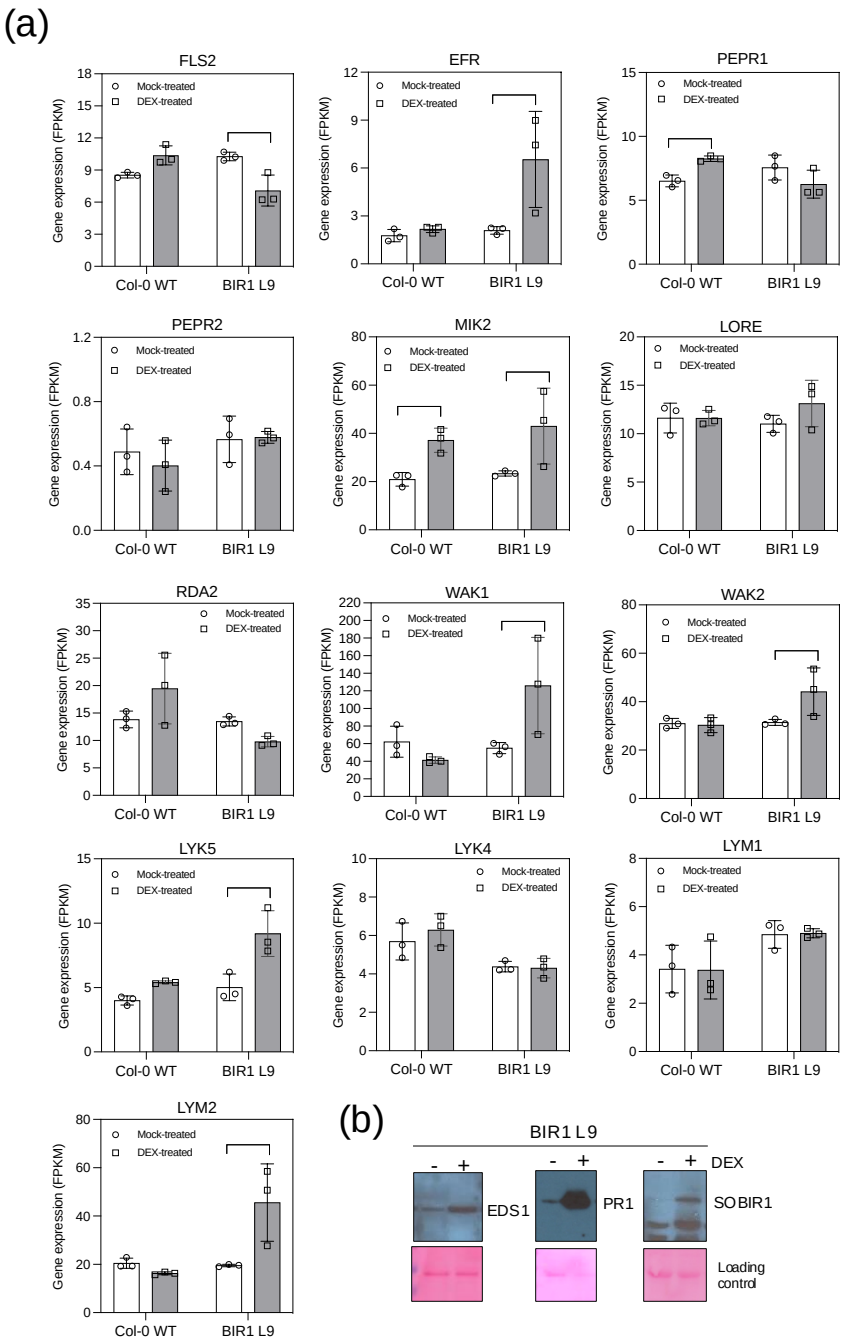

Figure S4

Differential expression of cell-surface pattern recognition receptors (PRR)-coding genes in *BIR1* overexpressing plants. **(a)** Relative expression levels are represented by the number of Fragments Per Kilobase of transcript sequence per Millions of base-pairs sequenced (FPKM) in each of the three independent samples per condition used for RNA-Seq. Significant differences between dexamethasone (DEX)- and mock-treated samples were analyzed using two-way ANOVA followed by Sidak´s multiple comparison test; *, adjusted *p*-value < 0.05. **(b)** Western blot analysis of EDS1, SOBIR1 and PR1 using specific antibodies. Plants were mock-treated (-) or DEX-treated (+) for 12 days. Protein loading control by Ponceau S is shown.

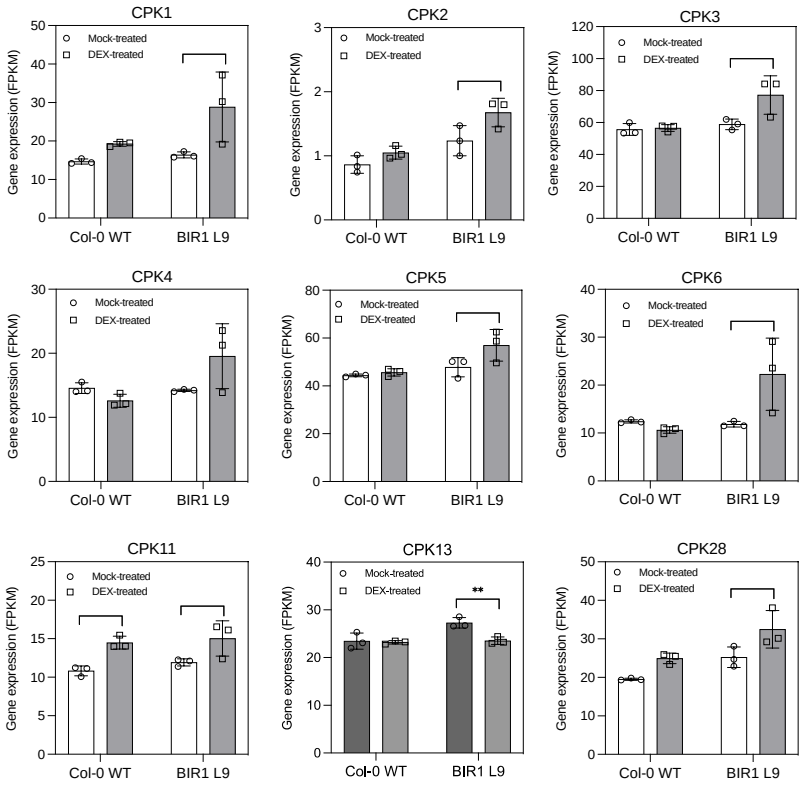

Figure S5

Differential expression of calcium-dependent protein kinases (CPK)-coding genes in *BIR1* overexpressing plants. Relative expression levels are represented by the number of Fragments Per Kilobase of transcript sequence per Millions of base-pairs sequenced (FPKM) in each of the three independent samples per condition used for RNA-Seq. Significant differences between dexamethasone (DEX)- and mock-treated samples were analyzed using two-way ANOVA followed by Sidak´s multiple comparison test; **, adjusted *p*-value < 0.01, *< 0.05.

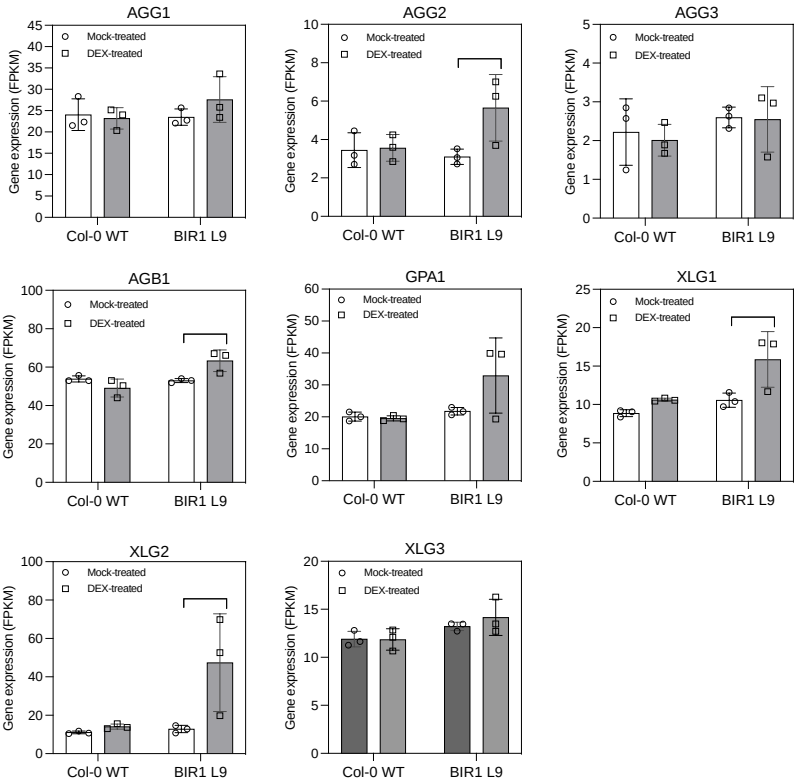

Figure S6

Differential expression of *HETEROTRIMERIC G PROTEIN* genes in *BIR1* overexpressing plants. Relative expression levels are represented by the number of Fragments Per Kilobase of transcript sequence per Millions of base-pairs sequenced (FPKM) in each of the three independent samples per condition used for RNA-Seq. Significant differences between dexamethasone (DEX)- and mock-treated samples were analyzed using two-way ANOVA followed by Sidak´s multiple comparison test; *, adjusted *p*-value < 0.05.

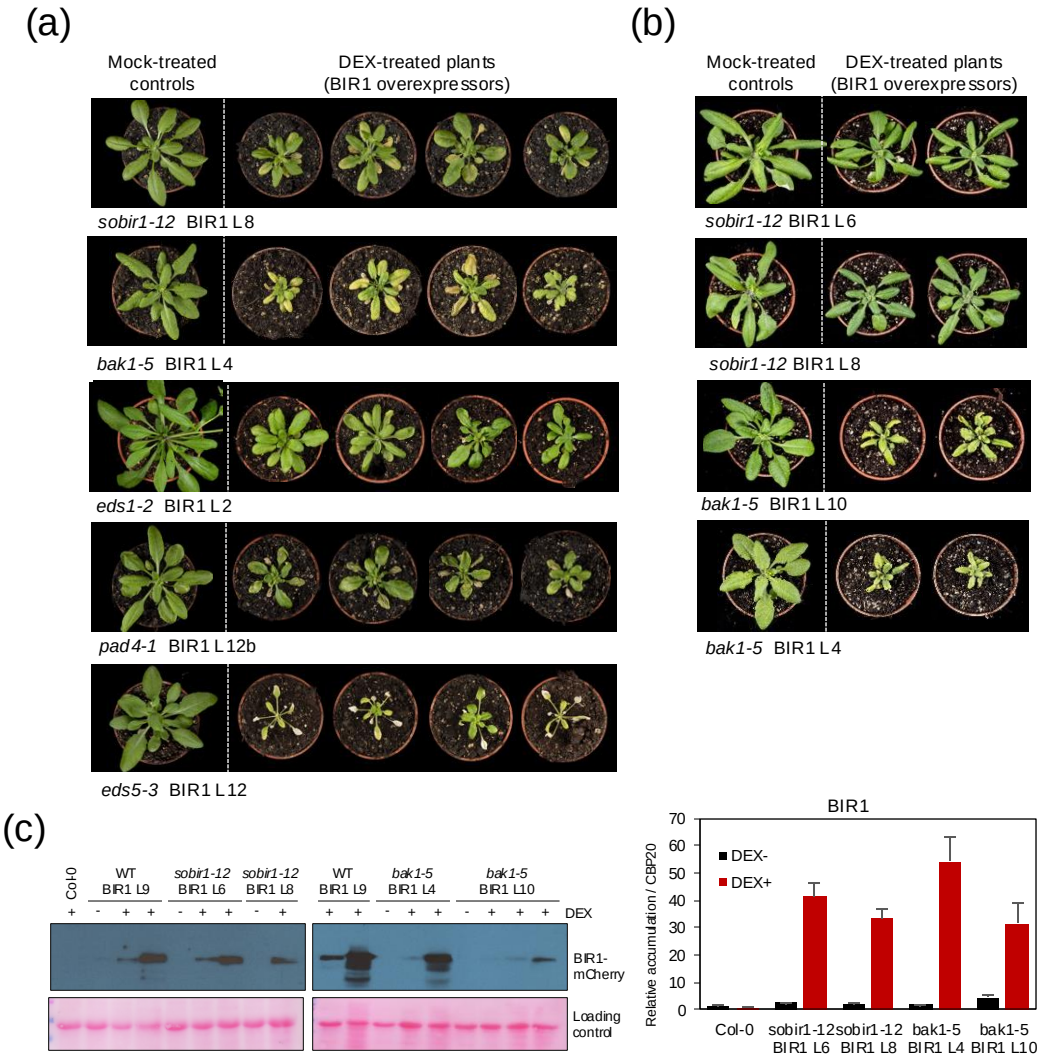

Figure S7

Morphological and growth defects in independent *BIR1* overexpressing plants of different immune mutant genetic backgrounds. **(a)** Morphology of representative dexamethasone (DEX)-inducible BIR1-mCherry transgenic Arabidopsis lines in *sobir1-12* (*sobir1-12* BIR1 L8), *bak1*-5 (*bak1*-5 BIR1 L4), *eds1*-2 (*eds1*-2 BIR1 L2), *pad4-1* (*pad4-1* BIR1 L12b) and *eds5-3* (*eds5-3* BIR1 L12) backgrounds. Photographs were taken after 10-12 days of 30 µM DEX treatment. Mock-treated plants are shown as controls. **(b)** Morphology and *BIR1* expression levels of DEX-treated and mock-treated *sobir1-12* BIR1 (L6, L8) and *bak1-5* BIR1 (L4, L10) plants as observed in a different repetition of the experiment. **(c)** Western blot analysis of BIR1-mCherry in the genotypes indicated. Plants were mock-treated (-) or DEX-treated (+) for 12 days. Protein loading control by Ponceau S is shown (left panel). qRT-PCR analysis showed comparable *BIR1* transcript levels in both genotypes. Each sample consisted of RNA pooled from six different plants (right panel).

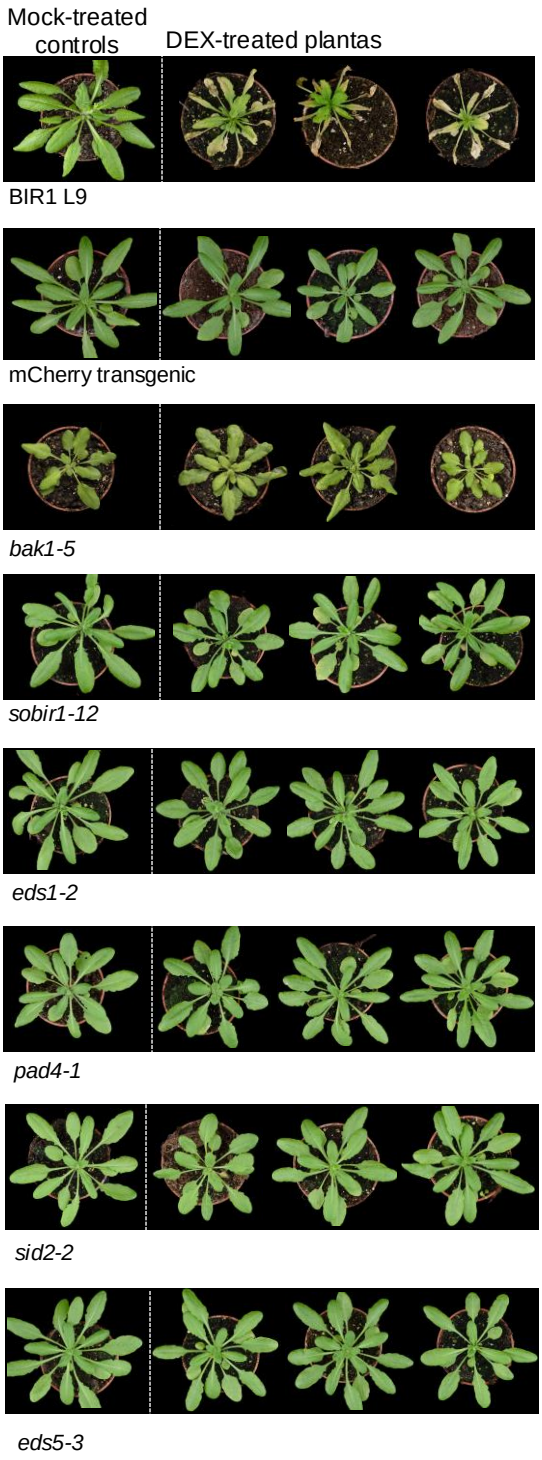

Figure S8

Morphological phenotypes of dexamethasone (DEX)-treated immune mutant genetic backgrounds and mCherry transgenic plants. Morphology of BIR1 L9, *sobir1-12*, *bak1*-5, *eds1*-2, *pad4-1*, *sid2-2* and *eds5-3* mutant plants and mCherry transgenic Arabidopsis after 12 days of treatment with 30 µM DEX. BIR1 L9 plants and mock-treated plants of each genotype are shown as controls.